Research Article

Franco Foresta Martin*, Silvio G. Rotolo, Manuela Nazzari, Maria Luisa Carapezza

Chlorine as a Discriminant Element to Establish the Provenance of Central Mediterranean Obsidians

Abstract: Chlorine is a minor element present in obsidians in quantities greater than in average igneous rocks. The chlorine concentration in obsidians is generally low, of the order of tenths of wt %, but it exhibits an appreciable differentiation among geological sources. Despite these characteristics, chlorine has rarely been taken into consideration as a possible indicator of obsidian provenance and it does not appear in the chemical analytical tables accompanying the geochemical characterisation of obsidian samples.

In this work, after an overview of chlorine geochemistry and cycle, we present thirty-one new electron microprobe (EPMA) analyses, including Cl, of geologic obsidians sampled from the four sources of the Central Mediterranean, exploited in prehistoric times (Monte Arci, Palmarola, Lipari and Pantelleria). The results are compared with 175 new EPMA analyses, including Cl, of archaeological obsidians already characterised in previous work and of known provenance. As such it was possible to ascertain that each source has a characteristic chlorine concentration, showing the utility of its use in the studies of obsidian provenance. Furthermore, given that the solubility of chlorine in silicate melts is correlated to its alkali content, in particular sodium, we assessed the efficacy of simple binary graphs Cl vs Na_2O to better constrain the provenance of the obsidian samples.

Keywords: Chlorine geochemistry, Central Mediterranean Obsidian, EPMA analyses, Obsidian-sources discrimination.

1 Introduction

In this work, we investigate the potential of chlorine (Cl), which is a minor constituent of silicate magmas, to establish the provenance of obsidians. This research aims to provide archaeometrists an analytical parameter that is, at the same time, easy to obtain through the most common non-destructive or partially-destructive elemental analyses (e.g. SEM-EDS, EPMA, XRF), and a reliable tracer in obsidian provenance studies.

Since the pioneering studies of the first half of the 1900s concerning the geochemistry of Cl, it has been ascertained that some silicic volcanic glasses have a content of this element significantly higher than that found in the average of igneous rocks. For example, in many rhyolitic obsidians, Cl exceeds 0.40% by weight, and in some peralkaline obsidians with a pantelleritic composition, it reaches 1 wt%, compared to an average of 0.02 wt% found in igneous rocks (Clark & Washington, 1924; Bowen, 1937; Kuroda & Sandell, 1953; Macdonald & Bailey, 1973; Lowenstern, 1994; Lanzo, Landi, & Rotolo, 2013). This feature is explained by the fact that Cl behaves like a highly incompatible element that tends to concentrate in low-temperature SiO_2-rich melts (residual melts after protracted crystal fractionation), rather than being fixed in the lattices of crystallizing minerals (although can substitute hydroxyl in micas and amphiboles). Therefore its concentration increases in the more evolved magmas, i.e. trachytes and rhyolites (Carroll, 2005; Bonifacie et al., 2008).

*Corresponding author: Franco Foresta Martin, Laboratorio Museo di Scienze della Terra Isola di Ustica (PA), Italy, E-mail: sidereus@rocketmail.com
Franco Foresta Martin, Silvio G. Rotolo, Istituto Nazionale di Geofisica e Vulcanologia, Sezione di Palermo, Italy
Silvio G. Rotolo, Dipartimento di Scienze della Terra e del Mare (DiSTeM), Università di Palermo, Italy
Manuela Nazzari, Maria Luisa Carapezza, Istituto Nazionale di Geofisica e Vulcanologia, Sezione di Roma 1, Italy

Experiments on silica-rich (felsic) melts have shown that Cl solubility rises with increasing concentration of network modifying cations, such as Na, K, Mg, Ca and Fe (Carroll & Webster, 1994 and references therein), with the result that Cl is much more soluble in a peralkaline (Na, K, and Fe-rich) rhyolitic melt such as a pantellerite melt (Carrol, 2005; Metrich & Rutherford, 1992; Carroll & Webster, 1994).

Comparatively to water, Cl is more soluble in silicic melts at low pressure (P< 2 kbar) with a well-known inverse correlation between its content and pressure: i.e. the lower P is, the higher Cl is solubility (Carroll, 2005; Metrich & Rurtherford, 1992; Signorelli & Carroll, 2002). It must be said that Cl solubility in silicic melts is much more complex than any other volatile phase, being strongly influenced by the possible coexistence of a solid (halite), fluid (H_2O-rich free volatile phase), or even a saline hydrous phase (brine). Besides the effects of pressure and melt composition (P-X) on Cl content, silicate melts (quenched as glasses) show a marked geographic variability, depending on the tectonic setting, as well as on the extent of the differentiation processes and evolution of magmas (Kuroda & Sandell, 1953; Macdonald, Smith, & Thomas, 1992), and can provide useful information on the volcano-genetic processes (Webster, 1997; Lanzo et al., 2013).

Starting from these considerations, this study aims to verify if Cl content, alone or associated with other major and minor elements, can be a useful parameter to discriminate the four obsidian sources exploited in prehistoric times in the Central Mediterranean area, namely Monte Arci (Sardinia), Palmarola (Latium), Lipari and Pantelleria (Sicily) (Figure 1) and then to develop a reliable and easy method of assessing obsidian provenance.

Figure 1: Location of the four obsidian sources exploited in prehistoric times in the Central Mediterranean area.

2 Background on Chlorine Geochemistry

A *cosmopolitan* chemical element which, like few others, possesses siderophilic, lithophilic, hydrophilic, and atmophilic properties: this is how Cl was defined as early as the middle of the twentieth century when its ubiquitous presence in the Solar System and terrestrial geospheres was recognised (Kuroda & Sandell, 1953). Chlorine is the twentieth natural element in order of abundance on the Earth lithosphere (Winterton, 2000), constituting a minor element in the rocks, but the geochemical studies developed in recent decades have highlighted its significant presence in the various terrestrial reservoirs and allowed estimations of its amounts and fluxes (Schilling, Unni, & Bender, 1978; Jarrad, 2003; Eggenkamp, 2014).

Like many other natural elements that we find on our planet, Cl was created by nuclear fusion processes and nucleosynthesis in the core of some massive and mature stars and then scattered in space when these stars ended their existence with a huge explosion (nova or supernova stages). In this way, Cl became part of the gas and dust nebula from which the Sun and the other bodies of our solar system were formed about 5 billion years ago through processes of coalescence, gravitational attraction, and collapse, according to the pillars of current cosmogonic theories (Urey, 1951; Burbidge, Burbidge, Fowler, & Hoyle, 1957). The estimation of the total mass of Cl in the Earth is based on the relative abundances of the elements measured in the CI[1] type carbonaceous chondrites, the most primitive and undifferentiated meteorites recovered on the Earth, which are considered as the building blocks of our solar system. Elemental abundances of the carbonaceous chondrites are substantially identical to those measured in the Sun absorption lines, and they reflect the composition of the primordial solar nebula (Cameron, 1973; Palme, Lodders, & Jones, 2014). The most updated assessments agree on the presence of 5.24×10^3 Cl atoms per 10^6 Si atoms (Eggenkamp, 2014). Knowing that Si represents about 15% of the weight of our planet (Press & Siever, 1978), the total terrestrial mass of Cl is estimated between 5.5 and 8.2×10^{20} kg (Sharp & Draper, 2013). In absolute value, the mass of the terrestrial Cl is therefore considerable, but if we consider its mean concentration on the entire terrestrial bulk, we obtain a value of just 10 ± 5 ppm (Eggenkamp, 2014).

The distribution of chlorine in the Earth is quite inhomogeneous, depending on various factors: the mass differentiation processes experienced by our planet during its early formation, the Cl chemical behaviour, and its transfer processes between the geospheres. As Cl is a very volatile element, it was mostly transferred from the inner reservoirs (mantle) to the surface (crust) and hence preferentially partitioned into the fluid phases (free fluid-phase coexistent with magma, atmosphere, oceans), which in the course of geological time generated also Cl rich sediments (evaporites), (Schilling, Unni, & Bender, 1978). The literature reports different estimates of the Cl partitioning in the terrestrial reservoirs, sometimes discordant when referring to the innermost geospheres, for which the evaluations are mostly conjectural. An updated review made by Eggenkamp (2014, and references therein) assigns 57% of the Cl total mass to the outermost Earth's layers, i.e. oceans 2.71×10^{19} kg; evaporites 1.89×10^{19} kg; sediments 3.78×10^{19} kg; continental crust 2.27×10^{18} kg; and oceanic crust 2.30×10^{17} kg. The remaining 43% of Cl terrestrial mass, i.e. $\sim 7 \times 10^{19}$ kg, would be placed in the mantle. The amount of Cl in the atmosphere is minimal compared to that of the other reservoirs, since it retains only 0.00000001% of the total Earth's Cl. The biggest uncertainties concern the content of Cl in the Earth's core, but it is commonly believed that it has very limited exchanges with the other geospheres and hence can be ignored when reconstructing the Earth's Cl cycle (Eggenkamp, 2014).

The identification of the transfer mechanisms between the various terrestrial reservoirs of Cl and the quantitative estimate of the fluxes engaged geochemists since the second half of the twentieth century. The pioneering work of Rubey (1951) established that halogens and other volatiles are concentrated on the Earth's surface in greater amounts than that produced only by the weathering processes, and hypothesized a substantial contribution from deep geological fluxes. These ideas developed on a more solid basis with the establishment of plate tectonics theory and the recognition that subduction, island arc volcanism, seafloor spreading, and hot spot volcanism constitute fundamental mechanisms for the transport of Cl (and other volatiles) from the mantle to the crust and vice versa (Eggenkamp, 2014).

The discovery of a major Cl reservoir in the lower mantle was recently claimed by Hanyu, Shimizu, Ushikubo, Kimura, Chang, Hamada, Motoo, Ikaru, and Ishikawa (2019). By analysing the olivine-hosted melt inclusions from ocean island basalt (OIB) rich in Cl and high in radiogenic Pb isotopes (^{206}Pb, ^{207}Pb, ^{208}Pb) they were able to reconstruct the behaviour of the Cl that sinks into the mantle with the subducting oceanic crust (Figure 2).

According to Hanyu et al. (2019), this subducting Cl partially returns to the surface through mechanisms of dehydration of the crust, triggering the partial melting of the above mantle wedge, originating thus arc magmatism. The rest of Cl, i.e. an estimated flux of the order of 10^9 kg/yr, sinks into the lower mantle, where a Cl amount of $0.6–1.2 \times 10^{19}$ kg accumulates (the same order of magnitude as that of the upper mantle). Through geological times, the Cl of the lower mantle is cycled back to the surface by means of the upwelling plumes of OIB which feed the intraplate volcanoes. The analysis of Pb isotopes associated with Cl was decisive in the evaluation of the very long time (billions of years) during which this deep geological cycle of Cl takes place (Hanyu et al., 2019).

---

1 In the abbreviation CI, C is for Carbonaceus, and I for Ivuna, the name of the Tanzania locality where in 1938 fell and was recovered the homonymous meteorite. After the analysis, the 705 g weight sample proved to be one of the rarest types of carbonaceous chondrite recovered on Earth.
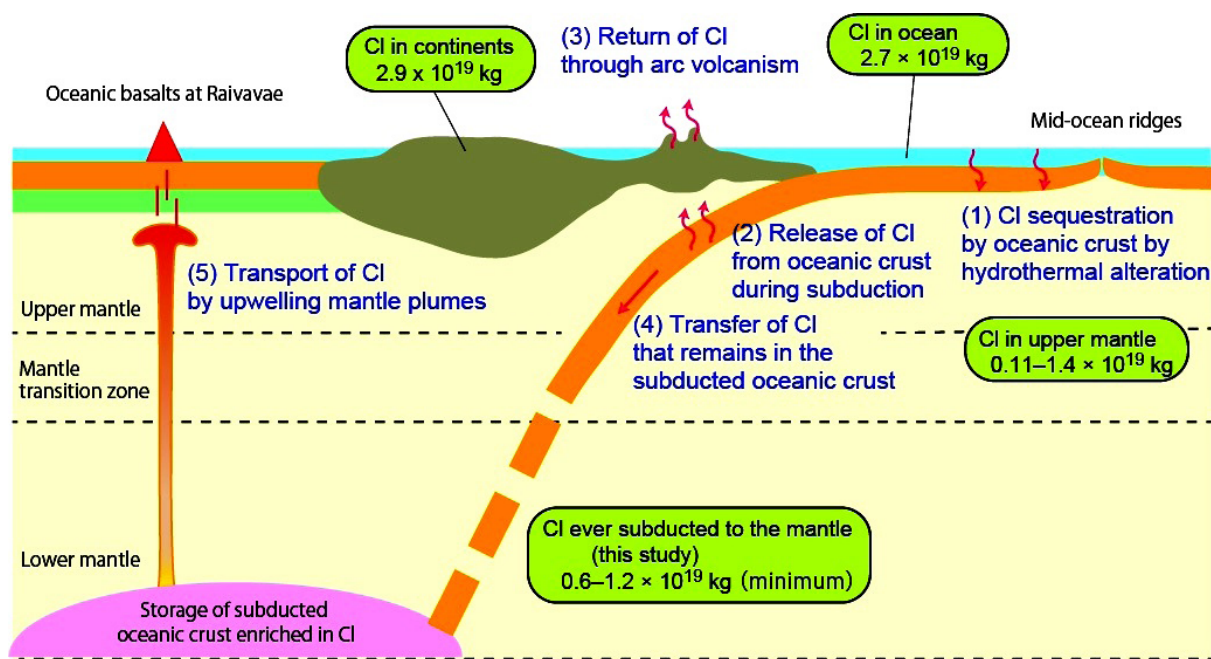
Figure 2: The Cl cycling from the oceanic crust to the surface, through the mantle. **(1)** The oceanic crust takes Cl from the seawater. **(2)** Cl is lost from the subducted oceanic crust under high temperature and pressure conditions. **(3)** Cl is returned to the surface through arc volcanism. **(4)** Small amounts of Cl remain and sink to form a Cl-rich reservoir in the lower mantle. **(5)** Cl-rich mantle material is transported by the upwelling of mantle plumes, generating Cl-rich ocean island basalts. Green ovals show the Cl in major Cl reservoirs. The minimum estimated Cl transported by subducted oceanic crust ($0.6–1.2 \times 10^{19}$ kg) is comparable to the Cl in the upper mantle. After Hanyu et al. (2019). Reproduced with Author's permission.

This brief review of the terrestrial Cl cycle aims to highlight how this element is redistributed in the various geospheres through volcanic processes, and that it is present in the magmas that ascend to the earth's surface, generating also silica-rich lavas, thus becoming an eligible element for the geochemical characterisation of obsidians.

3 The Search for Effective Obsidian Provenance Parameters

The seminal study by Cann and Renfrew (1964) on the characterisation of the obsidians through trace elements analysis represented a watershed in the provenance studies of these archaeological artifacts. Before it, the attribution of obsidian artifacts to specific geological sources relied essentially on the determination of the major and minor elements through ordinary chemical analyses, using more or less destructive methods. However, the results were often ambiguous. Although obsidians of different origins present some compositional differences in terms of major and minor elements, boundary lines between sources are not so sharp and overlaps can occur, making discrimination problematic. Cann and Renfrew (1964) cited as an example the paper of Cornaggia Castiglioni, Fussi and D'Agnolo (1962), who thought they could distinguish the obsidian sources of the Central Mediterranean through the relative differences of manganese and phosphorus content but, applying this method, they erroneously attributed to the geological sources of Melos (a Greek island in the Aegean Sea) some archaeological obsidians found at Malta. Later, thanks to the analysis of the trace elements, whose concentrations vary strongly from source to source, it emerged that Malta imported obsidians exclusively from the Italian islands of Lipari and Pantelleria (Cann & Renfrew, 1964; Hallam, Warren, & Renfrew, 1976).

For decades, after the innovative contribution of Cann and Renfrew (1964), the geochemical characterisation of obsidians has been dominated by the determination of trace elements, which offer the certainty of unambiguous sources attributions (Williams-Thorpe, 1995 and references therein). For the scholars engaged in obsidian sourcing, it has become a standard procedure to combine the analyses of the major-minor elements with those of the trace elements, to have a complete geochemical characterisation of the studied specimens (e.g. Barca, De Francesco, & Crisci, 2007; De

Francesco, Crisci, & Bocci, 2008; Glascock, Braswell, & Cobean, 1998; Gratuze, 1999; Tykot & Young, 1996; Tykot, 2002; Tykot, Setzer, Glascock, & Speakman, 2005).

More recently, some authors have proposed to perform provenance studies of obsidians only through the analysis of a few major and minor elements (SiO_2, Al_2O_3, Na_2O, K_2O, CaO, and possibly also Fe_2O_3 tot, TiO_2), relying on the latest generation of analytical instruments that guarantee better performances, as in the case of scanning electron microscope equipped with an energy dispersive detector (SEM-EDS), (Acquafredda, Andriani, Lorenzoni, & Zanettin, 1999; Le Bourdonnec, Bontempi, Marini, Mazet, Neuville, Poupeau, & Sicurani, 2010). In this way, the advantage comes from the possibility of analysing a large number of samples quickly and economically, and above all operating in a non-destructive way.

Some authors have highlighted the discriminating potential of alkalis, in particular of Na, in distinguishing the obsidian sources of the Central Mediterranean; indeed an increase of Na_2O concentrations can be observed in the sequence: Monte Arci, Lipari, Palmarola, Pantelleria (Le Bourdonnec, Poupeau, & Lugliè, 2006; Le Bourdonnec et al., 2010; Tykot, 2002). Le Bourdonnec et al. (2010) report the measurements made with SEM-EDS of over 100 geological samples of obsidians in which the concentration intervals of Na_2O (wt %) of the four Central Mediterranean sources are distinct, without overlapping: M. Arci, 2.47–3.25; Lipari, 3.60–3.71; Palmarola, 4.18–4.25; Pantelleria, 5.51–6.32. Even some Pantelleria subsources can be recognized: the Na_2O concentration of Balata dei Turchi obsidians is markedly higher (6.1–6.3 wt %) than that of the Lago di Venere (5.5–5.6 wt %), (Le Bourdonnec et al., 2010), although this outcrop remains poorly constrained on its field location.

On the other hand, the literature reports cases in which the provenance distinction via the mere Na_2O concentration is impossible. This is mainly due to weathering-related alkali loss, in particular, Na loss which occurs in archaeological samples in contact with the ground and exposed to washout phenomena; or also because of glass devitrification processes (Ewart, 1971 and references therein; Lipman, Christiansen, & Alstine, 1969). Examples of significant soda leaching can be found in some archaeological obsidians of the island of Lipari, where the Na concentration can drop by 1% and more below the average (Acquafredda & Muntoni, 2008; Italiano et al., 2018).

Table 1 summarises the compositional intervals of the major and minor elements usually measured for the geochemical characterisation of obsidians and highlights the possible compositional overlaps which might affect provenance attribution. In practice, only the obsidians of Pantelleria have concentrations of some elements (Na, Al, and especially Fe) typical exclusively of pantellerite rocks largely present on the island.

Table 1: Compositional intervals (min. – max. wt %) of major and minor elements in the obsidians of the four Central Mediterranean sources: M. Arci, Palmarola, Lipari, and Pantelleria, according to literature (Acquafredda et al., 1999; Acquafredda & Muntoni, 2008; De Francesco, Crisci, & Bocci, 2008; Le Bourdonnec et al., 2010; Tykot, 2002). Overlaps between sources are highlighted in gray.

SOURCE	SiO_2	Al_2O_3	Na_2O	K_2O	Fe_2O_3tot	CaO
M. ARCI	72.7–76.9	12–14.0	2.5–3.5	4.9–6.3	1.0 –2.2	0.5–1.1
LIPARI	74.2–76.0	12–13.7	2.6–4.5	5.4–7.6	1.3 –1.9	0.5–0.7
PALMAROLA	74.4–75.6	12.1–13.1	4.2–4.8	4.6–5.0	1.9–2.0	0.5
PANTELLERIA	69.2–75.0	6.7–10.7	5.5–6.3	4.2–4.8	7–9.8	0.2–0.5

When the study of obsidian provenance is entrusted only to major and minor elements, and the concentration of Na alone does not give univocal answers, the combined use of significant parameters and binary graphs is necessary. For example, it could be helpful to use binary graphs Al_2O_3 vs Na_2O/K_2O, proposed by Acquafredda et al. (1999) to discriminate between the compositionally contiguous and superimposable sources of Lipari and Monte Arci; or Al_2O_3 vs Fe_2O_3tot and Al_2O_3 vs CaO that, following Le Bourdonnec et al. (2010), could separate the four Monte Arci sub-sources.

The vast literature on characterisation and sourcing of the four Central Mediterranean obsidian outcrops exploited during prehistory attests that Cl has not been used as a parameter to distinguish among these sources. Despite Cl being detectable with the most widespread analytical methods (SEM, EPMA, XRF) in similar quantities over those of other minor elements such as Mn, Mg, and Ti, which are usually included among the analysed elements, it does not appear in the chemical tables of most papers. The literature also attests that some obsidian sources of the Carpathian Mountains

and Korea have been classified, regarding their provenance, based on boron and chlorine contents (in particular on concentration ratios B/SiO_2 vs Cl/SiO_2), obtained through Prompt Gamma Activation Analysis (PGGA), a non-destructive analytical method that requires the use of a neutron source for irradiating the obsidians and obtain gamma-ray spectra characteristic of the elemental composition (Kasztovszky & Biró, 2006; Kasztovszky, Biró, & Kis, 2014; Kasztovszky, et al., 2019; Jwa et al., 2018).

Our study aims to evaluate the effectiveness of Cl concentration measures for obsidian sourcing purposes, regarding the previously mentioned four sources of the Central Mediterranean, and using the most accessible and economical analytical techniques available for the determination of major and minor elements.

4 Materials and Method

4.1 Sampling

In order to test the discriminating ability of Cl content in determining the obsidian provenance, two distinct groups of samples were analysed in this study, one geological, and the other archaeological.

The geological group includes 31 samples representative of the four obsidian quarries exploited during prehistoric times in the Central Mediterranean area: Monte Arci, Palmarola, Lipari, and Pantelleria (Table 2).

Twelve samples originate from the volcanic massif of **Monte Arci** (central-western side of Sardinia), and precisely three for each of the four sub-sources indicated in the literature with the abbreviations SA, SB1, SB2, SC (Tykot, 1992, 2002). Six samples come from the island of **Lipari** (Aeolian Archipelago, Sicily): three from the most exploited *Vallone Gabellotto* quarry, and three from *Canneto Dentro*, both on the north-eastern side of the island. Six samples were collected on the island of **Palmarola** (Pontine Islands, Latium): three on the west coast at *Cala del Porto*, and three on the east coast at *La Radica*. And finally, seven samples come from the island of **Pantelleria** (Sicily channel): five from *Balata dei Turchi*, the most exploited obsidian quarry of the island in the southern coast; one from the nearby *Salto La Vecchia*; and one from *Fossa della Pernice*, in the north-central area of the island. Table 2 summarises the source, sub-source, and localisation of each sample.

The archaeological group is made of 175 samples belonging to the Parish Museum of the island of Ustica: most are flakes or debitages, only a few are tools as blades, arrows, bulins. They were collected in the middle of the last century by Carmelo Gaetano Seminara, the Honorary Inspector of the archaeological heritage of the island, during surface surveys carried out in areas of archaeological and historical importance, but without establishing specific correlations with prehistoric contexts. We can generically say that the ages of these obsidians range from the Neolithic to the Middle Bronze Age when the island of Ustica was intensely populated and frequented. The archaeological samples have already been the subject of archaeometric investigations that led to establishing their provenances (Foresta Martin et al., 2017).

4.2 Microchemical Analyses

The preparation of the samples for the chemical micro-analyses was done by detaching a small fragment from each obsidian. In geological samples, the detached fragments had a maximum size of 5 mm; in archaeological samples, to preserve their integrity as much as possible, the detached fragments had a maximum size of 3 mm. These fragments, gathered in groups of 6–10, were then embedded in epoxy resin stubs, abraded and polished. The resulting mounts were ultrasonically washed in bi-distilled water and then carbon-coated before performing the microprobe analyses.

The elemental composition of the obsidians was measured at the INGV laboratory in Rome. Microchemical analyses were performed using an electron probe micro-analyzer (EPMA) Jeol-JXA8200 combined EDS-WDS (equipped with five WD spectrometers). Data was collected using 15 kV accelerating voltage and 8 nA beam current. To avoid Na-migration under the electron beam, a slightly defocused beam (diameter ≤ 10 µm) was used, with a counting time of 5 s on the background and 10 s on the peak. The precision of the microprobe was evaluated through the analysis of well-characterised synthetic oxide and mineral secondary standards. The following standards have been adopted for the various chemical elements: albite (Si, Al, and Na), forsterite (Mg), augite (Fe), rutile (Ti), orthoclase (K), apatite (F, P, and Ca), sodalite (Cl), celestine (S) and rhodonite (Mn). Sodium and potassium were analysed first to further prevent

Table 2: Geological sample location. For each one, collecting place, source, sub-source, and coordinates are specified. Sample abbreviation: MAR = Monte Arci; LIP = Lipari; PALM = Palmarola; PANT = Pantelleria.

SAMPLE	SOURCE & SITE	SUB-SOURCE	COORDINATES
MAR SA 1602	MONTE ARCI (Conca 'e Cannas)	SA	39.721092 N; 8.731678 E
MAR SA 1606	MONTE ARCI (Conca 'e Cannas)	SA	39.721092 N; 8.731678 E
MAR SA 1610	MONTE ARCI (Conca 'e Cannas)	SA	39.721092 N; 8.731678 E
MAR SB1 1613	MONTE ARCI (M. Sparau)	SB1	39.7816547 N; 8.7185580 E
MAR SB1 1617	MONTE ARCI (M. Sparau)	SB1	39.7816547 N; 8.7185580 E
MAR SB1 1618	MONTE ARCI (M. Sparau)	SB1	39.7816547 N; 8.7185580 E
MAR SB2 1622	MONTE ARCI (Conca 'e Ollastu)	SB2	39.7634538 N; 8.6795184 E
MAR SB2 1624	MONTE ARCI (Conca 'e Ollastu)	SB2	39.7634538 N; 8.6795184 E
MAR SB2 1626	MONTE ARCI (Conca 'e Ollastu)	SB2	39.7634538 N; 8.6795184 E
MAR SC 1631	MONTE ARCI (Acqua Frida)	SC	39.801164 N; 8.740031 E
MAR SC 1633	MONTE ARCI (Acqua Frida)	SC	39.801164 N; 8.740031 E
MAR SC 1634	MONTE ARCI (Acqua Frida)	SC	39.801164 N; 8.740031 E
LIP1 GAB	LIPARI (Vallone del Gabellotto)	GABELLOTTO	38.496644 N; 14.949624 E
LIP2 GAB	LIPARI (Vallone del Gabellotto)	GABELLOTTO	38.496644 N; 14.949624 E
LIP3 GAB	LIPARI (Vallone del Gabellotto)	GABELLOTTO	38.496644 N; 14.949624 E
LIP1 CD	LIPARI (Canneto Dentro)	CANNETO	38.484938 N; 14.961476 E
LIP2 CD	LIPARI (Canneto Dentro)	CANNETO	38.484938 N; 14.961476 E
LIP3 CD	LIPARI (Canneto Dentro)	CANNETO	38.484938 N; 14.961476 E
PALM CDF 1702	PALMAROLA (Cala del Porto)	M. TRAMONTANA S-W	40.936554 N; 12.857377 E
PALM CDF 1703	PALMAROLA (Cala del Porto)	M. TRAMONTANA S-W	40.936554 N; 12.857377 E
PALM CDF 1705	PALMAROLA (Cala del Porto)	M. TRAMONTANA S-W	40.936554 N; 12.857377 E
PALM RAD 1502	PALMAROLA (La Radica)	LA RADICA	40.936554 N; 12.860207 E
PALM RAD 1504	PALMAROLA (La Radica)	LA RADICA	40.936554 N; 12.860207 E
PALM RAD 1505	PALMAROLA (La Radica)	LA RADICA	40.936554 N; 12.860207 E
PANT FP1 1050	PANTELLERIA (Zinedi)	FOSSA DELLA PERNICE	36.815000 N; 11.9802778 E
PANT BDT 1602	PANTELLERIA	BALATA DEI TURCHI	36.73635 N; 12.02225 E
PANT BDT 1604	PANTELLERIA	BALATA DEI TURCHI	36.7368 N; 12.021883 E
PANT BDT 1607	PANTELLERIA	BALATA DEI TURCHI	36.7364833 N; 12.016667 E
PANT BDT 1608	PANTELLERIA	BALATA DEI TURCHI	36.7366000 N; 12.021183 E
PANT BDT 1609	PANTELLERIA	BALATA DEI TURCHI	36.7367167 N; 12.0211 E
PANT SLV 0653	PANTELLERIA	SALTO LA VECCHIA	36.7372222 N; 12.007778 E

alkali migration. Based on counting statistics, analytical uncertainties relative to the reported concentrations indicate that precision was better than 5% for all cations.

Twelve major and minor elements were determined: SiO_2, TiO_2, Al_2O_3, FeOtot, MnO, MgO, CaO, Na_2O, K_2O, P_2O_5, Cl, F. For each obsidian piece, 9–16 measurements were made to avoid inhomogeneities due to the presence of microlites beneath the surface; the average values were then calculated.

5 Results and Discussion

5.1 Geochemical Classification of Samples

The major and minor element contents of the geological samples are presented in Table 3 and those of the archaeological samples in Table 4. The sum of oxides in all analysed geological and archaeological samples was over 97 wt %. For a more complete geochemical classification, we added some other chemical parameters to the tables: **PI** or *peralkalinity index*, is expressed by molar $(Na_2O+K_2O)/Al_2O_3$; **A/CNK,** *alumina saturation index*, is molar $Al_2O_3/(CaO+Na_2O+K_2O)$; **A/NK,** Shand (1927) index, is molar $Al_2O_3/(Na_2O+K_2O)$ (note that the latter is the PI inverse fraction).

The geological samples have been geochemically characterised for the first time in the present study. The archaeological samples were already geochemically characterized by Foresta Martin et al. (2017); their provenance was determined and it is reported in the "source" column of Table 4. For this study, the samples were re-analysed to determine their Cl content. Concerning the provenances, on a total of 175 archaeological samples, 152 (87%) have been attributed to Lipari; 21 (12%) to Pantelleria; 1 to Palmarola (UST-49); and one resulted to be a non-obsidian: it is UST-69, a fragment of an ancient high lime low alkali (HLLA) artificial glass of 17th–18th century AD, (Foresta Martin, Barca, & Posedi, 2020, this special issue). This latter sample was therefore discarded from Table 4 and related graphs.

The TAS classification diagram of igneous rocks, i.e. Total Alkali ($Na_2O + K_2O$) vs Silica (SiO_2) after Le Maitre et al. (2002) (Figure 3A and inset B), indicates that the obsidians analysed in this study, both the geological and archaeological samples, plot into the field of rhyolites, which are characterised by high silica (68–76 wt %) and alkali (8–12 wt %) contents; the only exception is the archaeological sample UST-10 which is a peralkaline trachyte from Pantelleria. Moreover, all the analysed samples fall in the field of alkaline magmas, according to Miyashiro classification (1978), but many Lipari and Monte Arci SA obsidians are very close to the sub-alkaline boundary.

The TAS diagram effectively separates only two large groups:

1. The mono-source group of Pantelleria obsidians (top left position in Figure 3B), which is relatively richer in alkali and poorer in silica, and characterised by peralkalinity index > 1.0. Note that archaeological samples (blue dots encompassed in blue ellipses) are more dispersed with respect to geological samples (red dots) and exhibit terms with lower alkali content. This is partly due to the greater variability related to a large number of archaeological samples analysed, but the effect of alkali loss because of weathering should also be considered, remembering that these are surface findings. In a previous study (Foresta Martin et al., 2017), these archeological samples were attributed to the Balata dei Turchi quarry, on the southern coast of Pantelleria. An outlier of this group is the UST-10 archaeological peralkaline trachytic sample, which exhibits the lowest SiO_2 content (66.93 wt %) and the highest alkali content (12.08 wt %). In literature, Pantelleria obsidians with similar chemical characteristics are reported by Francaviglia (1988, 2001) and by Tykot (1995) and attributed to quarries in the north of the island (Lago di Venere and Gelkhamar); but the existence and locations of these sub-sources are controversial, as explained by Rotolo, et al. (2020). We must conclude that archaeological obsidians of proven Pantellerian origin (certified by trace elements patterns) with a geochemical composition similar to UST-10 are still orphans of a certain source.

2. The multi-source group that piles together obsidians of Monte Arci, Lipari, and Palmarola, which are the richest in silica and the poorest in alkali (bottom right in Figure 3B) and characterised by a PI <1 or at most ≃1 (Palmarola case). The geological samples of this group (red dots) highlight contiguities and overlaps between Lipari and Monte Arci, whose SA sub-source (red ellipse at bottom right in Figure 3B) detaches from the other mixed SB1, SB2, and SC sub-sources, due to higher silica and lower alkali contents. The archaeological obsidians of this group all come from Lipari, except a single Palmarola sample (UST-49) that is the first from this island found until now in Sicily (Foresta Martin et al., 2017). The archaeological samples of Lipari are much more dispersed than the geological ones.

The TAS diagram is excellent for defining the chemical characteristics of the magmatic melts that generated the obsidians, but as evidenced in Figure 3B it is not suitable for distinguishing the provenances of archaeological samples, due to the contiguity and overlapping between the sources.

Table 3: Major and minor element wt % content of geological samples analyzed in this study. PI = peralkalinity index; A/CNK = alumina saturation index; A/NK = Shand (1927) index. Sample abbreviation as in Table 2.

SAMPLE	SiO$_2$	TiO$_2$	Al$_2$O$_3$	FeO tot	MnO	MgO	CaO	Na$_2$O	K$_2$O	P$_2$O$_5$	Cl	F	Na$_2$O + K$_2$O	PI	A/CNK	A/NK
MAR SA 1602	75.54	0.07	13.26	1.13	0.06	0.08	0.55	3.42	5.48	0.11	0.13	0.17	8.90	0.87	1.06	1.15
MAR SA 1606	75.89	0.10	13.11	1.04	0.05	0.06	0.51	3.41	5.45	0.08	0.14	0.15	8.85	0.88	1.06	1.14
MAR SA 1610	75.38	0.11	13.41	1.12	0.06	0.08	0.58	3.48	5.38	0.08	0.13	0.18	8.87	0.86	1.06	1.16
MAR SB1 1613	74.43	0.18	13.82	1.05	0.02	0.05	0.71	3.42	5.95	0.11	0.10	0.16	9.37	0.87	1.04	1.15
MAR SB1 1617	74.56	0.21	13.72	0.97	0.04	0.07	0.70	3.42	5.96	0.12	0.11	0.12	9.38	0.88	1.03	1.14
MAR SB1 1618	74.53	0.17	13.76	1.02	0.03	0.09	0.71	3.41	5.88	0.12	0.10	0.16	9.29	0.87	1.04	1.15
MAR SB2 1622	74.29	0.22	13.75	1.00	0.03	0.12	0.73	3.62	5.94	0.10	0.09	0.10	9.57	0.90	1.00	1.11
MAR SB2 1624	74.38	0.21	13.84	0.85	0.03	0.08	0.72	3.56	6.00	0.11	0.09	0.12	9.56	0.89	1.01	1.12
MAR SB2 1626	74.51	0.22	13.77	0.91	0.03	0.12	0.70	3.72	5.70	0.09	0.09	0.14	9.42	0.89	1.01	1.12
MAR SC 1631	73.58	0.30	13.99	1.26	0.04	0.18	0.83	3.26	6.18	0.14	0.08	0.15	9.44	0.86	1.03	1.16
MAR SC 1633	73.94	0.25	13.86	1.16	0.03	0.14	0.83	3.25	6.18	0.13	0.08	0.15	9.43	0.87	1.02	1.15
MAR SC 1634	74.22	0.27	13.75	0.90	0.03	0.07	0.72	3.23	6.48	0.10	0.09	0.14	9.71	0.90	1.01	1.11
LIP1 GAB	74.88	0.08	12.75	1.49	0.07	0.03	0.71	4.03	5.40	0.01	0.36	0.19	9.43	0.98	0.93	1.02
LIP2 GAB	74.79	0.07	12.75	1.57	0.05	0.04	0.72	4.08	5.38	0.01	0.35	0.18	9.46	0.98	0.92	1.02
LIP3 GAB	75.09	0.07	12.64	1.51	0.05	0.04	0.71	4.00	5.34	0.01	0.36	0.17	9.34	0.98	0.93	1.02
LIP1 CD	75.23	0.05	12.62	1.44	0.07	0.04	0.68	3.98	5.38	0.02	0.33	0.15	9.36	0.98	0.93	1.02
LIP. 2 CD	74.79	0.08	12.86	1.48	0.07	0.03	0.70	4.16	5.29	0.01	0.36	0.17	9.45	0.98	0.93	1.02
LIP. 3 CD	74.84	0.08	12.80	1.51	0.06	0.05	0.72	4.10	5.29	0.02	0.34	0.19	9.39	0.97	0.93	1.03
PALM. CDP. 1702	75.18	0.10	13.05	0.96	0.06	0.01	0.24	4.81	5.16	0.02	0.22	0.19	9.97	1.03	0.94	0.97
PALM. CDP 1703	75.05	0.11	13.12	0.97	0.07	0.01	0.23	4.81	5.22	0.02	0.21	0.18	10.03	1.03	0.94	0.97
PALM. CDP. 1705	75.03	0.07	13.05	1.06	0.08	0.03	0.31	4.73	5.21	0.03	0.22	0.17	9.94	1.03	0.93	0.97
PALM. RAD. 1502	74.96	0.09	13.04	1.10	0.05	0.02	0.26	4.78	5.24	0.02	0.22	0.22	10.02	1.04	0.93	0.96
PALM. RAD. 1504	74.54	0.10	12.95	1.49	0.09	0.04	0.46	4.78	5.15	0.02	0.21	0.16	9.93	1.04	0.91	0.96
PALM. RAD. 1505	74.59	0.08	12.98	1.49	0.09	0.04	0.44	4.73	5.15	0.02	0.20	0.20	9.87	1.03	0.92	0.97
PANT FP1 1050	70.45	0.50	10.61	5.73	0.29	0.21	0.36	6.32	4.86	0.05	0.36	0.23	11.19	1.48	0.65	0.68
PANT BDT 03 1602	72.50	0.19	7.66	6.71	0.28	0.03	0.24	7.41	4.15	0.03	0.49	0.27	11.56	2.18	0.45	0.46
PANT BDT 03 1604	71.87	0.21	7.44	7.51	0.31	0.03	0.24	7.21	4.31	0.02	0.50	0.31	11.52	2.22	0.44	0.45
PANT BDT 03 1607	72.20	0.21	7.46	7.06	0.29	0.03	0.24	7.34	4.22	0.03	0.49	0.38	11.56	2.23	0.44	0.45
PANT BDT 03 1608	72.17	0.22	7.59	7.04	0.30	0.03	0.23	7.16	4.38	0.02	0.52	0.31	11.54	2.18	0.45	0.46
PANT BDT 03 1609	72.39	0.21	7.76	6.73	0.26	0.03	0.24	7.29	4.26	0.03	0.50	0.27	11.55	2.14	0.46	0.47
PANT SLV 0653	71.65	0.21	7.47	7.63	0.32	0.03	0.24	7.28	4.31	0.03	0.51	0.28	11.59	2.23	0.44	0.45

Table 4: Major and minor element wt % content of archaeological samples analyzed in this study. PI = peralkalinity index; A/CNK = alumina saturation index; A/NK = Shand (1927) index. UST-69 sample was discarded because it resulted to be non-obsidian. LIP = Lipari; PANT = Pantelleria.

SAMPLE	SOURCE	SiO_2	TiO_2	Al_2O_3	FeO tot	MnO	MgO	CaO	Na_2O	K_2O	P_2O_5	Cl	F	$Na_2O + K_2O$	PI	A/CNK	A/NK
UST - 1	LIP	75.24	0.13	13.24	1.51	0.10	0.11	0.75	4.17	5.20	0.04	0.33	0.06	9.37	0.94	0.96	1.06
UST - 2	LIP	74.68	0.03	13.21	1.42	0.10	0.09	0.69	4.05	5.11	0.03	0.31	0.11	9.17	0.92	0.98	1.08
UST - 3	LIP	74.72	0.11	13.21	1.47	0.06	0.10	0.66	4.03	4.99	0.00	0.33	0.04	9.02	0.91	1.00	1.10
UST - 4	LIP	75.53	0.11	13.27	1.47	0.06	0.11	0.69	4.23	5.16	0.02	0.29	0.04	9.39	0.95	0.96	1.06
UST - 5	LIP	75.39	0.10	13.29	1.36	0.08	0.11	0.63	4.22	5.14	0.03	0.31	0.07	9.36	0.94	0.97	1.06
UST - 6	PANT	71.72	0.27	7.85	7.82	0.28	0.12	0.24	7.09	4.28	0.05	0.49	0.24	11.37	2.07	0.47	0.48
UST - 7	LIP	74.96	0.06	13.20	1.38	0.04	0.14	0.64	3.99	5.17	0.03	0.29	0.07	9.17	0.92	0.99	1.08
UST - 8	LIP	75.14	0.10	13.09	1.40	0.09	0.14	0.75	4.21	5.08	0.01	0.30	0.04	9.29	0.95	0.95	1.05
UST - 9	LIP	75.25	0.08	13.15	1.50	0.10	0.14	0.70	4.14	5.11	0.03	0.31	0.02	9.25	0.94	0.97	1.06
UST - 10	PANT	66.93	0.64	11.51	7.70	0.32	0.25	0.54	7.42	4.66	0.06	0.26	0.11	12.08	1.50	0.63	0.67
UST - 11	LIP	74.62	0.14	12.95	1.49	0.07	0.12	0.64	4.06	5.00	0.00	0.33	0.06	9.06	0.93	0.98	1.07
UST - 12	LIP	74.39	0.06	12.98	1.46	0.07	0.10	0.67	4.05	5.12	0.03	0.31	0.03	9.16	0.94	0.97	1.06
UST - 13	LIP	75.15	0.08	12.94	1.38	0.06	0.07	0.66	4.03	4.87	0.07	0.33	0.07	8.90	0.92	0.99	1.09
UST - 14	LIP	75.04	0.09	13.04	1.47	0.07	0.13	0.70	4.12	5.08	0.04	0.30	0.03	9.20	0.94	0.96	1.06
UST - 15	LIP	74.50	0.08	12.97	1.51	0.05	0.08	0.74	4.17	5.08	0.05	0.32	0.07	9.25	0.95	0.95	1.05
UST - 16	LIP	74.79	0.14	13.15	1.56	0.07	0.14	0.74	4.13	5.08	0.05	0.32	0.05	9.22	0.94	0.96	1.07
UST - 17	LIP	75.92	0.09	13.25	1.40	0.10	0.14	0.68	4.09	5.17	0.02	0.30	0.02	9.26	0.93	0.98	1.07
UST - 18	PANT	71.38	0.20	7.74	7.60	0.36	0.07	0.27	7.11	4.59	0.03	0.50	0.17	11.70	2.15	0.45	0.46
UST - 19	LIP	74.99	0.09	13.15	1.50	0.08	0.13	0.71	4.07	5.04	0.02	0.31	-	9.11	0.92	0.98	1.08
UST - 20	LIP	75.56	0.11	12.84	1.44	0.06	0.10	0.66	3.67	5.40	0.02	0.30	0.05	9.07	0.93	0.98	1.08
UST - 21	PANT	71.89	0.27	7.80	7.87	0.37	0.09	0.24	6.99	4.37	0.02	0.50	0.13	11.36	2.08	0.47	0.48
UST - 22	LIP	74.82	0.08	12.96	1.45	0.09	0.12	0.68	4.02	5.07	0.02	0.32	0.05	9.09	0.93	0.97	1.07
UST - 23	LIP	74.48	0.07	12.99	1.55	0.06	0.14	0.70	4.08	5.25	0.03	0.33	0.03	9.33	0.95	0.95	1.05
UST - 24	LIP	75.08	0.12	13.05	1.43	0.06	0.09	0.72	4.10	5.13	0.03	0.31	0.06	9.23	0.94	0.96	1.06
UST - 25	LIP	75.24	0.05	13.08	1.44	0.11	0.10	0.74	4.12	5.13	0.01	0.32	0.14	9.25	0.94	0.96	1.06
UST - 26	LIP	75.38	0.11	13.15	1.43	0.05	0.11	0.71	4.13	4.97	0.04	0.29	0.05	9.10	0.93	0.98	1.08
UST - 27	LIP	75.40	0.09	13.19	1.55	0.09	0.13	0.75	4.15	5.12	0.02	0.31	0.11	9.27	0.94	0.96	1.07
UST - 28	LIP	75.50	0.10	13.25	1.41	0.14	0.10	0.75	4.06	5.12	0.05	0.30	0.06	9.18	0.92	0.98	1.08
UST - 29	LIP	75.29	0.07	13.12	1.50	0.05	0.10	0.70	4.01	5.01	0.04	0.33	0.04	9.02	0.92	0.99	1.09
UST - 30	LIP	75.58	0.07	13.13	1.46	0.07	0.12	0.76	4.05	5.06	0.03	0.29	0.09	9.11	0.92	0.97	1.08
UST - 31	LIP	75.21	0.10	13.30	1.47	0.07	0.10	0.74	4.13	5.06	0.02	0.32	0.05	9.19	0.92	0.98	1.08
UST - 32	LIP	75.95	0.09	13.09	1.40	0.10	0.08	0.68	4.03	5.06	0.03	0.33	0.09	9.09	0.93	0.98	1.08
UST - 33	PANT	71.64	0.26	7.82	7.79	0.34	0.06	0.24	7.04	4.08	0.03	0.42	0.17	11.11	2.05	0.48	0.49
UST - 34	LIP	74.67	0.09	13.13	1.46	0.07	0.15	0.72	3.98	5.03	0.06	0.30	0.03	9.01	0.91	0.99	1.09
UST - 35	LIP	75.89	0.11	13.23	1.19	0.07	0.09	0.69	3.96	5.34	0.03	0.28	0.13	9.30	0.93	0.98	1.07

_{Continued}**Table 4:** Major and minor element wt % content of archaeological samples analyzed in this study. PI = peralkalinity index; A/CNK = alumina saturation index; A/NK = Shand (1927) index. UST-69 sample was discarded because it resulted to be non-obsidian. LIP = Lipari; PANT = Pantelleria.

SAMPLE	SOURCE	SiO_2	TiO_2	Al_2O_3	FeO tot	MnO	MgO	CaO	Na_2O	K_2O	P_2O_5	Cl	F	Na_2O + K_2O	PI	A/CNK	A/NK
UST - 36	LIP	76.03	0.12	13.30	1.47	0.06	0.11	0.71	4.18	5.03	0.02	0.30	0.11	9.21	0.93	0.98	1.08
UST - 37	LIP	75.00	0.10	13.02	1.54	0.09	0.13	0.71	4.07	4.90	0.05	0.34	0.03	8.97	0.92	0.98	1.08
UST - 38	LIP	74.70	0.08	12.98	1.53	0.07	0.08	0.69	4.03	5.11	0.01	0.35	0.03	9.13	0.94	0.97	1.07
UST - 39	LIP	76.01	0.06	12.88	1.38	0.08	0.10	0.66	3.97	5.16	0.03	0.33	0.06	9.12	0.94	0.97	1.06
UST - 40	PANT	72.38	0.20	7.89	7.84	0.29	0.10	0.27	6.78	4.17	0.02	0.51	0.25	10.95	1.99	0.49	0.50
UST - 41	LIP	75.37	0.08	13.21	1.45	0.06	0.12	0.72	4.06	5.02	0.01	0.31	0.03	9.08	0.92	0.99	1.09
UST - 42	LIP	76.19	0.10	13.29	1.13	0.06	0.11	0.63	4.13	5.36	0.07	0.29	0.01	9.48	0.95	0.97	1.05
UST - 43	LIP	75.46	0.14	13.02	1.50	0.10	0.09	0.71	3.84	5.61	0.02	0.32	0.09	9.45	0.95	0.95	1.05
UST - 44	LIP	76.06	0.09	13.37	1.45	0.06	0.09	0.68	4.20	5.11	0.03	0.32	0.08	9.32	0.93	0.98	1.07
UST - 45	LIP	75.84	0.08	13.27	1.46	0.05	0.14	0.67	4.13	5.20	-	0.30	0.06	9.33	0.94	0.97	1.07
UST - 46	LIP	75.58	0.10	13.14	1.44	0.06	0.12	0.75	3.93	5.37	0.02	0.33	0.06	9.30	0.93	0.96	1.07
UST - 47	LIP	76.29	0.16	13.20	1.57	0.11	0.09	0.74	4.24	5.09	0.02	0.34	0.04	9.33	0.95	0.95	1.06
UST - 48	PANT	72.86	0.23	7.96	7.66	0.34	0.10	0.19	7.04	4.48	0.05	0.51	0.29	11.52	2.06	0.47	0.48
UST - 49	PALM	75.86	0.05	13.56	1.28	0.09	0.08	0.32	4.75	5.17	0.04	0.22	0.08	9.92	0.99	0.97	1.01
UST - 50	LIP	76.07	0.09	13.13	1.48	0.04	0.12	0.72	4.01	5.00	0.04	0.32	0.05	9.01	0.91	0.99	1.09
UST - 51	LIP	74.68	0.06	13.10	1.42	0.08	0.11	0.67	3.90	5.28	0.04	0.30	0.04	9.18	0.93	0.98	1.08
UST - 52	LIP	75.14	0.04	13.10	1.48	0.15	0.11	0.70	3.93	5.12	-	0.31	0.05	9.05	0.92	0.99	1.09
UST - 53	LIP	74.71	0.06	13.13	1.46	0.12	0.10	0.71	3.96	5.15	0.02	0.30	0.12	9.11	0.92	0.98	1.09
UST - 54	LIP	75.23	0.13	13.02	1.45	0.06	0.10	0.66	3.93	5.13	0.03	0.30	0.07	9.06	0.92	0.98	1.08
UST - 55	LIP	74.59	0.11	12.95	1.50	0.10	0.09	0.71	4.01	5.13	0.02	0.27	0.01	9.15	0.94	0.96	1.06
UST - 56	PANT	71.46	0.22	7.88	7.75	0.31	0.08	0.24	6.53	4.29	0.02	0.51	0.17	10.81	1.95	0.50	0.51
UST - 57	LIP	74.37	0.10	12.79	1.50	0.09	0.12	0.68	3.92	5.11	0.04	0.30	0.07	9.03	0.94	0.97	1.07
UST - 58	LIP	74.96	0.07	13.09	1.37	0.08	0.07	0.69	4.01	5.13	0.05	0.31	0.02	9.14	0.93	0.98	1.08
UST - 59	LIP	75.14	0.13	13.00	1.47	0.07	0.10	0.69	3.99	5.15	0.04	0.32	0.03	9.14	0.93	0.97	1.07
UST - 60	LIP	74.60	0.12	12.98	1.47	0.05	0.10	0.73	4.03	5.06	0.02	0.34	0.04	9.09	0.93	0.97	1.07
UST - 61	PANT	71.24	0.24	7.68	7.82	0.35	0.12	0.23	6.95	4.34	0.03	0.49	0.25	11.29	2.10	0.46	0.48
UST - 62	LIP	74.97	0.12	13.00	1.49	0.07	0.10	0.73	3.92	5.06	0.00	0.33	0.03	8.98	0.92	0.98	1.09
UST - 63	LIP	75.39	0.06	12.91	1.43	0.10	0.10	0.69	3.91	5.14	0.02	0.29	0.07	9.05	0.93	0.97	1.08
UST - 64	LIP	75.03	0.06	12.93	1.36	0.11	0.10	0.68	3.98	5.18	0.02	0.29	0.04	9.16	0.94	0.97	1.06
UST - 65	LIP	74.93	0.11	12.93	1.50	0.02	0.12	0.67	3.98	5.14	0.05	0.31	0.04	9.11	0.94	0.97	1.07
UST - 66	LIP	75.18	0.10	13.10	1.46	0.05	0.11	0.72	4.04	5.24	0.03	0.30	0.05	9.29	0.94	0.96	1.06
UST - 67	LIP	75.14	0.04	12.96	1.54	0.04	0.09	0.67	4.00	5.12	0.05	0.28	0.05	9.11	0.93	0.97	1.07
UST - 68	LIP	75.27	0.15	13.11	1.40	0.07	0.08	0.69	3.92	5.18	0.03	0.28	0.05	9.10	0.92	0.98	1.09
UST - 70	LIP	75.23	0.12	12.98	1.35	0.06	0.10	0.71	3.85	5.37	0.01	0.31	0.06	9.22	0.94	0.97	1.07
UST - 71	LIP	75.72	0.10	13.11	1.52	0.07	0.10	0.67	4.05	5.24	0.02	0.30	0.01	9.29	0.94	0.97	1.06

Continued**Table 4:** Major and minor element wt % content of archaeological samples analyzed in this study. PI = peralkalinity index; A/CNK = alumina saturation index; A/NK = Shand (1927) index. UST-69 sample was discarded because it resulted to be non-obsidian. LIP = Lipari; PANT = Pantelleria.

SAMPLE	SOURCE	SiO_2	TiO_2	Al_2O_3	FeO tot	MnO	MgO	CaO	Na_2O	K_2O	P_2O_5	Cl	F	$Na_2O + K_2O$	PI	A/CNK	A/NK
UST - 72	LIP	74.82	0.11	12.92	1.53	0.10	0.12	0.72	4.01	5.05	0.03	0.32	-	9.06	0.93	0.97	1.07
UST - 73	LIP	75.07	0.11	13.00	1.49	0.08	0.12	0.72	3.90	5.34	0.02	0.31	0.01	9.24	0.94	0.96	1.07
UST - 74	LIP	75.35	0.08	13.00	1.53	0.07	0.11	0.71	4.00	5.11	0.02	0.33	0.01	9.11	0.93	0.97	1.07
UST - 75	LIP	74.90	0.09	13.04	1.47	0.11	0.13	0.75	4.00	5.16	0.01	0.28	0.05	9.16	0.93	0.96	1.07
UST - 76	LIP	75.01	0.11	12.89	1.59	0.05	0.12	0.70	3.92	5.24	0.03	0.32	-	9.16	0.94	0.96	1.06
UST - 77	PANT	71.55	0.16	7.71	7.79	0.32	0.13	0.20	6.82	4.49	0.02	0.42	0.23	11.31	2.09	0.47	0.48
UST - 78	PANT	72.21	0.19	7.64	7.81	0.29	0.12	0.23	6.83	4.18	0.02	0.43	0.17	11.01	2.06	0.47	0.48
UST - 79	LIP	75.23	0.11	12.91	1.48	0.05	0.10	0.70	3.91	5.06	0.04	0.30	0.01	8.98	0.92	0.98	1.08
UST - 80	PANT	71.56	0.19	7.79	7.85	0.35	0.06	0.23	6.80	4.71	0.03	0.49	0.16	11.51	2.09	0.47	0.48
UST - 81	LIP	75.03	0.10	12.69	1.34	0.04	0.10	0.70	3.84	5.01	0.02	0.29	-	8.85	0.92	0.98	1.08
UST - 82	PANT	71.62	0.25	7.77	7.83	0.32	0.10	0.29	6.84	4.23	0.03	0.50	0.16	11.07	2.04	0.48	0.49
UST - 83	LIP	74.59	0.06	12.86	1.41	0.08	0.11	0.72	3.98	5.02	0.02	0.31	0.00	8.99	0.93	0.97	1.07
UST - 84	LIP	74.06	0.12	12.93	1.52	0.10	0.08	0.71	3.89	5.07	0.02	0.30	0.06	8.96	0.92	0.98	1.09
UST - 85	PANT	71.46	0.19	7.67	7.34	0.31	0.11	0.20	6.68	4.67	0.02	0.53	0.21	11.35	2.09	0.47	0.48
UST - 86	LIP	74.86	0.06	12.93	1.48	0.03	0.11	0.72	3.91	5.17	0.01	0.31	0.04	9.08	0.93	0.97	1.07
UST - 87	LIP	75.58	0.09	12.87	1.47	0.09	0.09	0.71	3.88	5.15	0.02	0.30	0.02	9.03	0.93	0.97	1.08
UST - 88	LIP	75.16	0.11	12.90	1.45	0.09	0.11	0.72	3.99	5.01	0.03	0.32	0.05	9.00	0.93	0.97	1.08
UST - 89	LIP	75.04	0.12	13.00	1.39	0.11	0.09	0.73	4.02	5.07	0.03	0.30	0.01	9.08	0.93	0.97	1.07
UST - 90	LIP	75.06	0.08	13.12	1.48	0.10	0.09	0.73	3.90	5.13	0.00	0.31	0.05	9.03	0.91	0.99	1.10
UST - 91	LIP	74.91	0.10	12.92	1.42	0.09	0.11	0.68	3.91	5.09	-	0.29	0.13	9.00	0.92	0.98	1.08
UST - 92	LIP	74.66	0.10	12.97	1.48	0.05	0.12	0.69	3.86	5.29	0.03	0.33	0.01	9.15	0.93	0.97	1.07
UST - 93	LIP	75.08	0.10	12.84	1.51	0.09	0.13	0.68	3.90	5.26	0.02	0.30	0.05	9.16	0.94	0.96	1.06
UST - 94	LIP	74.67	0.10	12.84	1.47	0.04	0.12	0.70	3.90	5.12	0.01	0.31	0.04	9.02	0.93	0.97	1.07
UST - 95	LIP	74.32	0.12	12.90	1.50	0.14	0.09	0.70	3.78	5.09	0.06	0.30	0.04	8.87	0.91	0.99	1.10
UST - 96	PANT	71.91	0.21	7.27	7.94	0.34	0.12	0.24	6.74	4.37	0.02	0.56	0.19	11.11	2.18	0.45	0.46
UST - 97	LIP	75.13	0.07	12.96	1.28	0.13	0.11	0.68	4.03	5.20	0.02	0.28	0.08	9.24	0.95	0.96	1.06
UST - 98	LIP	75.60	0.08	12.96	1.41	0.05	0.12	0.69	4.00	5.19	0.05	0.30	0.04	9.19	0.94	0.96	1.06
UST - 99	LIP	75.10	0.06	12.80	1.48	0.11	0.12	0.72	3.97	5.16	0.02	0.31	0.07	9.13	0.95	0.95	1.06
UST - 100	LIP	75.35	0.14	12.96	1.39	0.08	0.08	0.66	3.90	5.30	0.03	0.31	0.04	9.19	0.94	0.97	1.07
UST - 101	LIP	75.87	0.09	13.21	1.39	0.04	0.11	0.78	4.03	5.06	0.03	0.33	-	9.09	0.92	0.98	1.09
UST - 102	LIP	76.34	0.13	13.34	1.32	0.04	0.13	0.65	3.74	5.97	0.01	0.29	0.09	9.71	0.95	0.97	1.06
UST - 103	LIP	75.07	0.07	13.17	1.54	0.09	0.12	0.69	4.02	5.03	0.04	0.30	0.03	9.05	0.92	0.99	1.09
UST - 104	PANT	72.11	0.24	7.77	7.94	0.31	0.11	0.27	7.11	4.24	0.04	0.52	0.15	11.36	2.10	0.46	0.48
UST - 105	LIP	76.30	0.08	13.06	1.53	0.10	0.12	0.66	4.07	5.20	0.03	0.31	0.07	9.27	0.94	0.97	1.06
UST - 106	LIP	75.73	0.09	13.33	1.50	0.08	0.09	0.72	4.11	5.14	0.02	0.32	0.05	9.26	0.93	0.98	1.08

Continued **Table 4:** Major and minor element wt % content of archaeological samples analyzed in this study. PI = peralkalinity index; A/CNK = alumina saturation index; A/NK = Shand (1927) index. UST-69 sample was discarded because it resulted to be non-obsidian. LIP = Lipari; PANT = Pantelleria.

SAMPLE	SOURCE	SiO_2	TiO_2	Al_2O_3	FeO tot	MnO	MgO	CaO	Na_2O	K_2O	P_2O_5	Cl	F	Na_2O + K_2O	PI	A/CNK	A/NK
UST-107	LIP	75.09	0.04	12.98	1.38	0.12	0.10	0.61	4.00	5.18	0.04	0.32	0.02	9.18	0.94	0.98	1.06
UST-108	LIP	75.63	0.08	13.17	1.48	0.06	0.12	0.74	4.13	5.11	0.04	0.32	0.05	9.23	0.94	0.96	1.07
UST-109	LIP	75.54	0.08	13.39	1.45	0.06	0.09	0.71	4.27	4.99	-	0.32	0.02	9.26	0.93	0.98	1.08
UST-110	LIP	75.78	0.13	13.23	1.50	0.10	0.12	0.70	4.05	5.28	0.03	0.31	0.05	9.34	0.94	0.97	1.07
UST-111	LIP	75.73	0.12	13.14	1.45	0.09	0.09	0.69	4.07	5.06	0.03	0.31	0.02	9.14	0.93	0.98	1.08
UST-112	PANT	71.97	0.25	7.93	7.63	0.30	0.10	0.22	6.86	4.71	0.03	0.46	0.20	11.57	2.07	0.47	0.48
UST-113	LIP	75.69	0.06	13.33	1.35	0.14	0.12	0.71	4.01	5.07	0.00	0.29	0.00	9.08	0.91	1.00	1.10
UST-114	LIP	75.39	0.08	12.91	1.41	0.08	0.11	0.69	4.05	5.23	0.04	0.32	0.05	9.28	0.96	0.95	1.05
UST-115	LIP	75.58	0.08	13.14	1.48	0.07	0.09	0.70	4.06	5.05	0.04	0.30	0.04	9.11	0.92	0.98	1.08
UST-116	LIP	75.11	0.09	13.23	1.45	0.12	0.10	0.70	4.14	5.04	0.02	0.32	0.04	9.18	0.93	0.98	1.08
UST-117	LIP	74.87	0.04	13.11	1.33	0.06	0.11	0.67	4.06	5.08	0.02	0.29	0.06	9.14	0.93	0.98	1.07
UST-118	LIP	75.18	0.08	13.23	1.48	0.09	0.12	0.73	4.10	5.09	0.03	0.33	0.05	9.18	0.93	0.97	1.08
UST-119	LIP	75.33	0.08	13.20	1.43	0.08	0.11	0.72	4.13	5.17	0.05	0.31	0.11	9.30	0.94	0.96	1.06
UST-120	LIP	75.34	0.11	12.96	1.24	0.08	0.09	0.66	4.04	5.17	0.03	0.33	0.04	9.21	0.94	0.96	1.06
UST-121	LIP	75.01	0.11	13.20	1.54	0.12	0.10	0.64	4.05	5.08	0.03	0.31	0.03	9.13	0.92	0.99	1.08
UST-122	LIP	75.04	0.09	13.17	1.46	0.05	0.08	0.73	4.11	5.13	0.00	0.30	0.04	9.23	0.93	0.97	1.07
UST-123	LIP	75.05	0.06	13.09	1.28	0.08	0.09	0.68	3.99	5.06	0.02	0.29	0.04	9.04	0.92	0.99	1.09
UST-124	LIP	73.77	0.10	13.07	1.49	0.07	0.12	0.69	4.02	4.95	0.04	0.32	0.03	8.97	0.92	0.99	1.09
UST-125	LIP	73.26	0.09	12.90	1.43	0.07	0.10	0.70	3.96	4.97	-	0.30	0.09	8.93	0.92	0.98	1.08
UST-126	PANT	71.77	0.26	7.78	7.78	0.36	0.10	0.28	6.78	4.20	0.02	0.51	0.15	10.98	2.02	0.48	0.50
UST-127	LIP	74.40	0.10	12.87	1.50	0.06	0.11	0.73	3.92	4.97	0.05	0.32	0.05	8.89	0.92	0.98	1.09
UST-128	LIP	75.19	0.12	12.83	1.46	0.06	0.11	0.69	4.00	5.15	-	0.31	0.06	9.15	0.95	0.96	1.05
UST-129	LIP	75.30	0.08	13.02	1.48	0.06	0.12	0.75	4.02	5.15	0.01	0.29	0.07	9.17	0.94	0.96	1.07
UST-130	LIP	74.65	0.07	13.02	1.50	0.09	0.13	0.72	3.85	5.09	0.02	0.31	0.07	8.94	0.91	0.99	1.10
UST-131	LIP	74.63	0.10	12.87	1.48	0.07	0.10	0.72	3.96	5.07	0.01	0.31	0.11	9.04	0.93	0.97	1.07
UST-132	LIP	75.11	0.10	13.03	1.43	0.12	0.09	0.69	4.00	5.19	0.06	0.28	0.02	9.19	0.94	0.97	1.07
UST-133	LIP	75.13	0.11	12.95	1.24	0.09	0.11	0.68	3.99	5.17	0.01	0.25	-	9.16	0.94	0.97	1.06
UST-134	LIP	74.78	0.07	12.91	1.43	0.07	0.09	0.71	3.90	5.22	0.03	0.30	0.08	9.12	0.93	0.97	1.07
UST-135	LIP	74.92	0.10	12.91	1.32	0.07	0.11	0.66	3.84	5.16	0.03	0.29	0.03	9.00	0.92	0.99	1.08
UST-136	LIP	74.91	0.10	13.11	1.49	0.10	0.10	0.72	4.04	5.10	0.06	0.34	0.06	9.15	0.93	0.97	1.08
UST-137	PANT	71.30	0.22	7.80	7.64	0.29	0.11	0.26	6.61	4.31	0.02	0.52	0.20	10.93	1.99	0.49	0.50
UST-138	LIP	74.39	0.08	12.89	1.55	0.06	0.10	0.75	3.95	5.22	-	0.30	0.01	9.17	0.94	0.95	1.06
UST-139	LIP	74.24	0.10	12.94	1.49	0.08	0.13	0.70	4.08	5.14	0.05	0.29	0.07	9.22	0.95	0.96	1.05
UST-140	LIP	74.15	0.07	12.91	1.56	0.08	0.08	0.67	3.94	5.12	-	0.33	0.06	9.06	0.93	0.98	1.07
UST-141	LIP	74.57	0.06	13.11	1.27	0.08	0.11	0.68	4.01	5.18	0.02	0.25	0.05	9.19	0.93	0.98	1.07

_{Continued}**Table 4:** Major and minor element wt % content of archaeological samples analyzed in this study. PI = peralkalinity index; A/CNK = alumina saturation index; A/NK = Shand (1927) index. UST-69 sample was discarded because it resulted to be non-obsidian. LIP = Lipari; PANT = Pantelleria.

| SAMPLE	SOURCE	SiO_2	TiO_2	Al_2O_3	FeO tot	MnO	MgO	CaO	Na_2O	K_2O	P_2O_5	Cl	F	Na_2O + K_2O	PI	A/CNK	A/NK
UST - 142	LIP	73.95	0.12	12.74	1.31	0.07	0.15	0.71	3.87	5.06	0.02	0.32	0.06	8.93	0.93	0.97	1.07
UST - 143	LIP	73.92	0.12	13.02	1.48	0.09	0.12	0.64	3.93	5.10	0.03	0.31	0.07	9.03	0.92	0.99	1.09
UST - 144	LIP	74.56	0.07	12.97	1.44	0.08	0.09	0.68	3.79	5.14	0.04	0.32	0.04	8.93	0.91	0.99	1.10
UST - 145	LIP	74.71	0.09	12.92	1.31	0.07	0.12	0.67	4.00	5.13	0.01	0.30	-	9.12	0.94	0.97	1.06
UST - 146	LIP	74.35	0.11	12.99	1.49	0.07	0.09	0.68	3.67	5.76	0.04	0.30	0.08	9.43	0.95	0.96	1.06
UST - 147	LIP	73.90	0.07	12.91	1.51	0.08	0.08	0.68	3.99	5.06	0.03	0.32	0.06	9.05	0.93	0.97	1.07
UST - 148	LIP	74.63	0.11	12.74	1.41	0.04	0.10	0.76	3.69	5.47	0.07	0.31	0.04	9.17	0.94	0.95	1.06
UST - 149	LIP	74.76	0.11	12.78	1.46	0.06	0.10	0.69	3.98	5.07	0.05	0.30	0.06	9.05	0.94	0.96	1.06
UST - 150	LIP	74.41	0.12	12.81	1.33	0.10	0.08	0.70	3.81	5.20	0.05	0.29	0.09	9.01	0.93	0.97	1.08
UST - 151	LIP	75.26	0.14	13.00	1.35	0.10	0.12	0.70	3.89	5.11	0.04	0.32	0.05	9.00	0.92	0.98	1.09
UST - 152	LIP	74.08	0.08	12.78	1.48	0.08	0.09	0.69	3.93	5.08	0.01	0.34	0.07	9.02	0.94	0.97	1.07
UST - 153	PANT	71.40	0.25	7.82	7.82	0.31	0.08	0.26	6.54	4.47	0.02	0.53	0.23	11.01	2.00	0.49	0.50
UST - 154	LIP	74.72	0.12	13.09	1.34	0.05	0.12	0.62	3.93	5.19	0.00	0.29	0.06	9.13	0.92	0.99	1.08
UST - 155	LIP	74.54	0.10	12.84	1.27	0.07	0.10	0.67	3.87	5.10	0.05	0.29	0.07	8.97	0.93	0.98	1.08
UST - 156	LIP	73.89	0.04	12.63	1.17	0.07	0.10	0.49	3.94	4.99	0.04	0.34	0.01	8.92	0.94	0.99	1.06
UST - 157	LIP	74.74	0.09	13.07	1.41	0.07	0.10	0.68	3.96	5.18	0.02	0.31	0.11	9.15	0.93	0.98	1.08
UST - 158	LIP	74.23	0.06	12.88	1.54	0.10	0.09	0.67	4.00	5.15	0.04	0.30	0.09	9.15	0.94	0.96	1.06
UST - 159	LIP	74.45	0.10	13.04	1.53	0.06	0.08	0.64	3.86	5.48	0.01	0.31	0.08	9.34	0.94	0.97	1.06
UST - 160	LIP	74.12	0.08	13.06	1.49	0.10	0.12	0.72	3.94	5.05	0.02	0.31	0.09	8.99	0.91	0.98	1.09
UST - 161	LIP	75.03	0.10	12.82	1.58	0.08	0.10	0.73	3.96	5.17	0.04	0.34	0.08	9.13	0.94	0.95	1.06
UST - 162	LIP	74.47	0.08	12.84	1.49	0.09	0.07	0.67	3.90	5.30	0.03	0.32	0.09	9.20	0.95	0.96	1.06
UST - 163	LIP	74.39	0.09	12.87	1.33	0.06	0.11	0.72	3.90	5.06	-	0.33	-	8.96	0.92	0.98	1.08
UST - 164	LIP	74.21	0.09	12.89	1.52	0.05	0.11	0.79	3.95	5.13	0.03	0.32	0.07	9.08	0.94	0.96	1.07
UST - 165	PANT	70.43	0.21	7.66	7.78	0.39	0.12	0.25	6.89	4.36	0.03	0.51	0.17	11.25	2.10	0.46	0.48
UST - 166	LIP	74.22	0.11	12.95	1.48	0.05	0.11	0.72	4.05	5.00	0.04	0.31	0.07	9.05	0.93	0.97	1.07
UST - 167	LIP	74.19	0.09	13.03	1.55	0.06	0.12	0.73	3.99	5.05	0.01	0.32	0.05	9.04	0.92	0.97	1.08
UST - 168	LIP	74.82	0.10	13.17	1.51	0.10	0.11	0.74	3.97	5.06	0.01	0.31	0.09	9.03	0.91	0.99	1.10
UST - 169	LIP	74.40	0.11	12.83	1.42	0.07	0.09	0.68	3.94	5.09	0.04	0.30	0.07	9.02	0.93	0.97	1.07
UST - 170	LIP	74.52	0.12	12.78	1.34	0.10	0.10	0.67	4.05	5.28	0.02	0.30	0.05	9.33	0.97	0.94	1.03
UST - 171	LIP	74.30	0.12	12.76	1.44	0.13	0.11	0.70	3.93	5.13	0.04	0.30	0.05	9.06	0.94	0.96	1.06
UST - 172	LIP	75.15	0.09	13.25	1.48	0.09	0.10	0.70	4.00	5.12	0.05	0.32	0.02	9.12	0.92	0.99	1.09
UST - 173	LIP	74.97	0.08	12.91	1.47	0.08	0.09	0.66	3.96	5.16	0.04	0.32	0.09	9.11	0.94	0.97	1.07
UST - 174	LIP	73.95	0.08	12.83	1.43	0.07	0.10	0.70	3.95	5.12	0.04	0.32	0.07	9.07	0.94	0.96	1.07
UST - 175	LIP	74.21	0.09	12.93	1.47	0.04	0.10	0.72	3.74	5.55	0.03	0.28	0.10	9.28	0.94	0.96	1.06
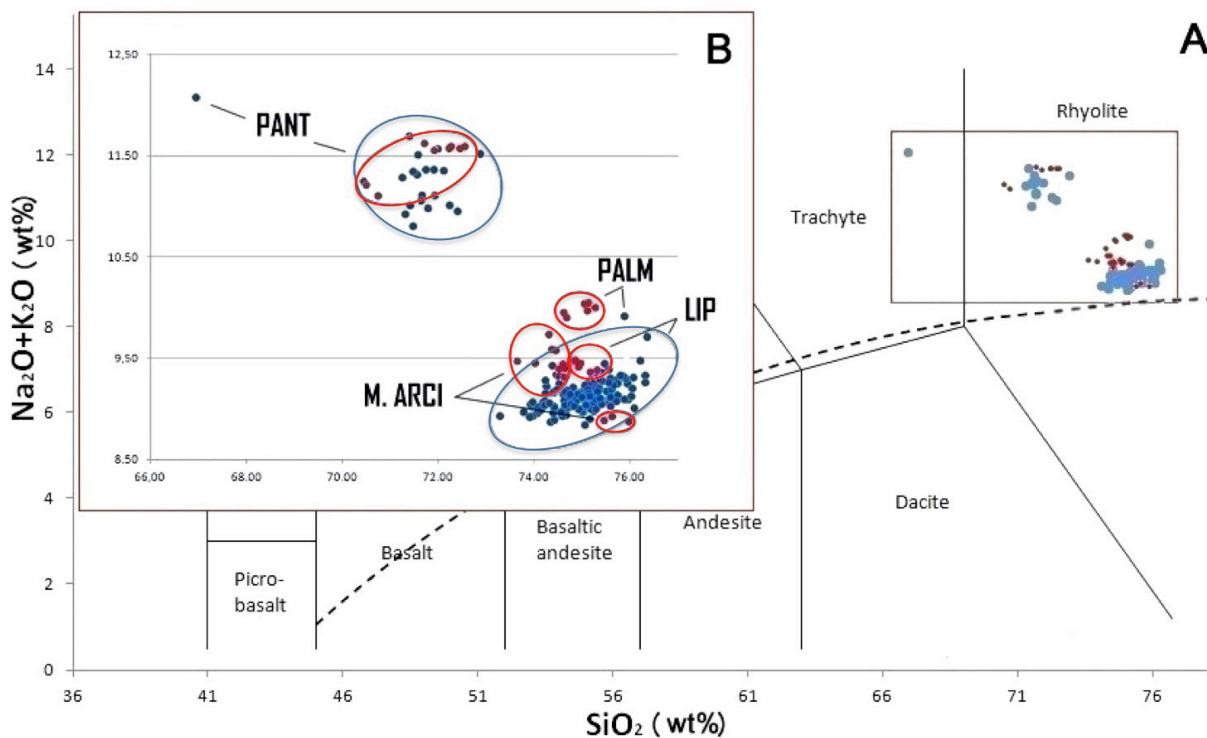
Figure 3: A) Total alkali vs silica diagram of geological (red dots) and archaeological (blue dots) obsidian samples. Classification fields after Le Maitre et al. (2002). In diagram A the dashed line is the boundary between alkaline (up) and subalkaline (down) magmas, after Miyashiro (1978). In the inset **B,** the red ellipses define the fields of geological samples; the blue ellipses the fields of archeological samples. PANT = Pantelleria, PALM = Palmarola, LIP = Lipari.

Obsidians can also be classified based on Shand's (1927) diagram A/CNK vs A/NK, which establishes the relationship between alumina (the second most abundant constituent of igneous rocks), alkalis and calcium. *Peraluminous*, or alumina oversaturated, are obsidians with A/CNK > 1, i.e. $Al_2O_3 > (CaO + Na_2O + K_2O)$. In a magmatic melt, this condition predisposes to the formation of Al-rich minerals such as feldspars. Even in volcanic glass such as obsidians, although the crystallisation process was inhibited by rapid cooling and high melt viscosity, microlites (< 50 microns) immersed in the glassy groundmass can be found and might become a source-discrimination factor (Acquafredda et al., 1999; Acquafredda & Paglionico, 2004). *Metaluminous*, i.e. alumina-poor obsidians have A/CNK < 1 and A/NK > 1, i.e.: $Al_2O_3 < (CaO + Na_2O + K_2O)$ and $Al_2O_3 > (Na_2O + K_2O)$. *Peralkaline* obsidians, have an alkali excess over alumina (PI > 1.0) and consequently are also alumina-poor (A/CNK < 1).

All three of these compositional categories are represented in the analysed obsidians as it can be appreciated from the A/CNK vs A/NK classification plot (Figure 4), with discrimination fields according to Maniar and Piccoli (1989). *Peraluminous* are the obsidians of Monte Arci characterised by an alumina saturation index just over 1; in particular, the obsidians of the SB2 sub-source are placed on the line corresponding to 1. *Metaluminous* are the obsidians of Lipari, which also in this diagram show a marked dispersion of the archaeological samples compared to the geological ones. *Peralkaline* are the obsidians of Pantelleria: this diagram also clearly distinguishes between those of the southern subsources (Balata dei Turchi, BDT and Salto La Vecchia, SLV) with the highest peralkalinity values, and the northern ones (Fossa della Pernice, FDP) less peralkaline. At last, the obsidians of Palmarola lie on the border between the *metaluminous* and *peralkaline* fields (Figure 4).

The petrographic, geochemical, and geologic characteristics of the four Central Mediterranean obsidian sources are summarized in Table 5.
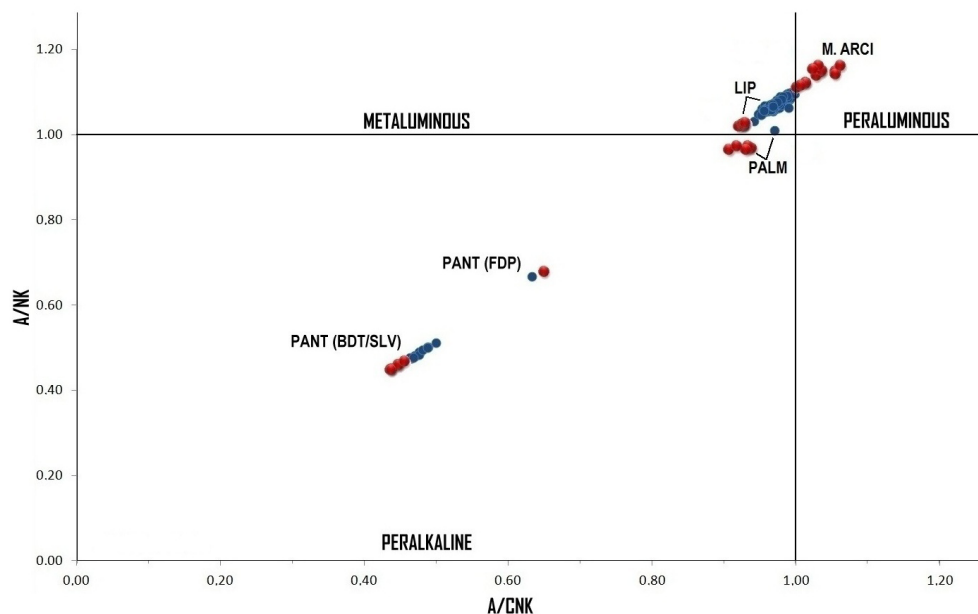
Figure 4: The Shand (1927) diagram A/CNK [molar ratio $Al_2O_3/(CaO+Na_2O+K_2O)$] vs A/NK [molar ratio $Al_2O_3/(Na_2O+K_2O)$] to classify obsidians based on their alumina content respect to alkalies and calcium. Discrimination fields after Maniar and Piccoli (1989). In red geological samples, in blue archeological samples. LIP = Lipari; PALM = Palmarola; PANT (FDP) = Pantelleria (Fossa Della Pernice); PANT (BDT/SLV) = Pantelleria (Balata Dei Turchi/Salto La Vecchia).

Table 5: Petrographic, geochemical and geological characteristics of the four Central Mediterranean obsidian sources.

LOCALITY	SUB-SOURCES	PETROGRAPHIC CLASSIFICATION	MAGMA SERIES	GEOLOGICAL AGE	GEOLOGICAL SETTING	REFERENCES*
MONTE ARCI	SA SB1 SB2 SC	PERALUMINOUS RHYOLITES	CALC-ALKALINE; MILDLY ALKALIC	3.6–3.2 Ma	WITHIN-PLATE	Tykot, 1992, 2002; **Montanini & Villa, 1993; Bellot-Gurlet et al., 1999**
PALMAROLA	MONTE TRAMONTANA	METALUMINOUS RHYOLITES	ALKALINE; PERALKALINE	1.6–1.7 Ma	WITHIN-PLATE; SUBDUCTION RELATED	**Barberi, Borsi, Ferrara, & Innocenti, 1967; Bellot-Gurlet et al, 1999;** Cadoux, Pinti, Aznar, Chiesa, & Gillot, 2005
LIPARI	GABELLOTTO CANNETO DENTRO	METALUMINOUS RHYOLITES	CALC-ALKALINE	11.4 ka–8.6 ka - - -	SUBDUCTION RELATED	**Bigazzi & Bonadonna, 1973; Arias, Bigazzi, & Bonadonna, 1980;** Forni et al., 2013; **Zanchetta et al., 2011;** Donato et al., 2017
PANTELLERIA	BALATA DEI TURCHI SALTO LA VECCHIA FOSSA PERNICE	PERALKALINE RHYOLITES TRACHITES	PERALKALINE	127–257 ka - - - 71–190 ka	WITHIN-PLATE	**Bigazzi, et al., 1971; Radi, Bigazzi, & Bonadonna, 1972;** Jordan et al., 2018; Rotolo et al., 2020.

*In bold, the papers containing radiometric age determinations of obsidian deposits.

5.2 Chlorine Compositional Ranges and Differentiation Among Sources

The geological samples of our collection show an appreciable variation of Cl content, covering the range 0.08–0.51 wt %, with good differentiation among the sources, as shown by Figure 5. From the lowest to the highest, the compositional intervals of Cl vary according to the sequence: Monte Arci, 0.08–0.14 wt %; Palmarola, 0.20–0.22 wt %; Lipari, 0.33–0.36 wt %; Pantelleria, 0.36–0.51 wt %. In this sequence, there is a clear *hiatus* between the sources of Monte Arci and Palmarola, and between Palmarola and Lipari, whereas a possible overlap exists between Lipari and Pantelleria due to the low Cl content (0.36 wt %) of Fossa della Pernice sample (PANT FP1 1050) with respect to the Cl values of others Pantelleria subsources, i.e. Balata dei Turchi and Salto La Vecchia (0.49–0.52 wt %) (Table 3). This anomaly is not surprising: Fossa della Pernice obsidian exhibits also lower values of silica, sodium, calcium, iron, and peralkalinity index, but higher of alumina, with respect to the other sub-sources of Pantelleria (Table 3).
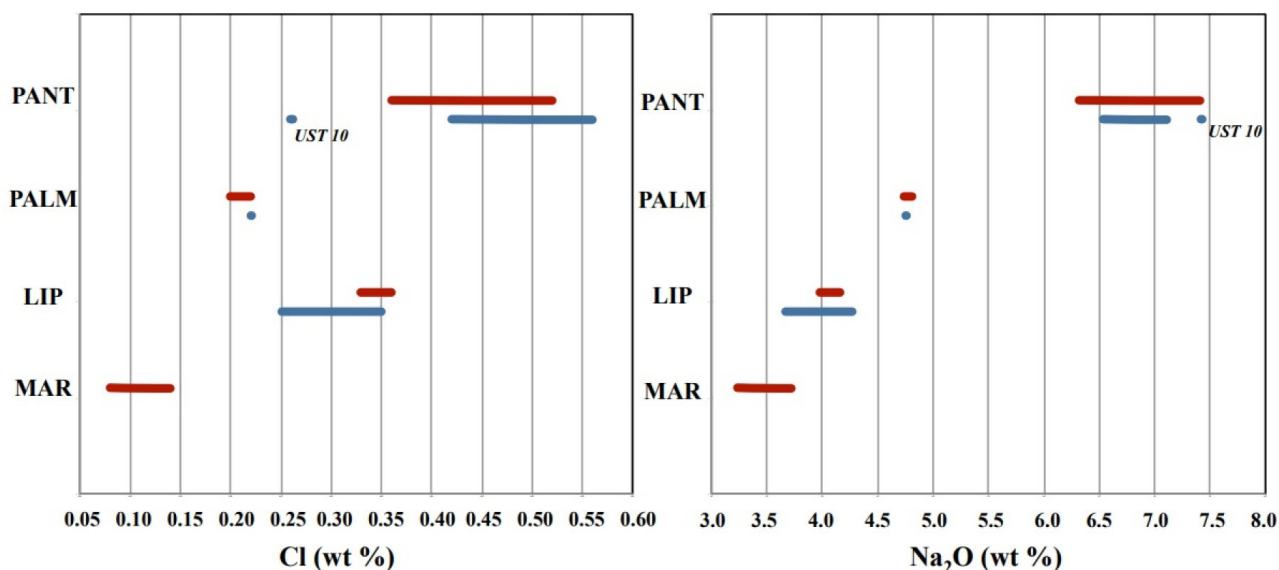
Figure 5: Variation ranges of Cl and Na_2O contents in samples representative of four geological obsidian sources in the Central Mediterranean (red) and in the 174 archaeological samples (blue) of known provenance collected at Ustica (Foresta Martin et al., 2017). Abbreviations: MAR = Monte Arci; PALM = Palmarola; LIP = Lipari; PANT = Pantelleria. UST 10 is an archeological peralkaline trachytic obsidian from Pantelleria source. Red bars = geological samples, blue bars = archeological samples.

In Figure 5, the Cl variation ranges of the obsidian archaeological samples (collected at Ustica) of known provenances show that:
- The single sample, source Palmarola, Cl = 0.22 wt %, fits with the geological samples of the same island;
- The large group of 152 samples, source Lipari, Cl = 0.25–0.35 wt %, comprises several samples with Cl content lower than in the corresponding geological samples;
- The 20 samples, source Pantelleria, Cl = 0.42–0.56 wt % shows a good correspondence with the geological obsidians, with slightly higher minimum and maximum values;
- The UST-10, peralkaline trachyte, source Pantelleria (unknown sub-source) detaches from the Pantelleria variation range because of its relatively low Cl content (0.26 wt %), which falls in the Lipari range; its Na_2O content (7.42 wt %) leads it back to the Pantelleria obsidians.

The ability of Cl in discriminating between obsidian sources is similar to that of Na_2O, which exhibits an analogous increasing sequence of values, with discrete intervals between the various sources, as it can be seen in Figure 5. The Na_2O content of our geological samples ranges from 3.23 to 7.41 wt %. From the lowest to the highest, the compositional intervals of Na_2O varies according to the sequence: Monte Arci, 3.23–3.72 wt %; Lipari 3.98–4.16 wt %; Palmarola, 4.73–

4.81 wt %; Pantelleria, 6.32–7.41 wt %. In this growing Na_2O sequence there is an inversion between the sources of Lipari and Palmarola, compared to the Cl sequence (Figure 5). The decoupling of the positive correlation Cl-Na for the latter two groups of samples may have many explanations, from small magma compositional variation to a pressure effect, and their interplay.

As to the archaeological samples, from Figure 5 it is clear that:

– The group of 152 samples, source Lipari, Na_2O = 3.67–4.27 wt %, covers the range of the geological samples extending beyond it, mostly on the side of the lower values, which partly overlap the Monte Arci geological samples (we do not have archeological samples from Monte Arci);
– The single UST-49 sample, source Palmarola, Na_2O = 4.75 wt %, coincides with the Palmarola geological range;
– The group of 21 samples, source Pantelleria, Na_2O = 6.53–7.42 wt %, falls within the geological obsidian range of the same island. This group includes also the UST-10 peralkaline trachytic sample, which shows the highest Na_2O content.

The attitude of Cl and Na to discriminate obsidian sources depends on the geochemical relationships between these two elements. As already mentioned, Cl solubility in magmas rises with increasing content of network modifying cations and especially Na (Lowenstern, 1994). This correlation explains the increasing sequence of Cl and Na_2O shown in Figure 5.

The correlations existing between Cl and the principal network modifying cations, i.e. Na, K, Mg, Ca are presented in Figure 6. Cl has good positive correlations with Na_2O (R^2= 0.75) and PI (R^2= 0.72) and a moderate correlation with Na_2O + K_2O (R^2= 0.61); it shows a strong negative correlation with K_2O (R^2= −0.81), and a low negative correlation with CaO (R^2= −0.37) and MgO (R^2= −0.10).

Among these binary graphs, there are at least a couple capable of making a clear distinction between the four obsidian sources in the Central Mediterranean, without ambiguities caused by excessive dispersion of values and overlaps. In our opinion, the most effective purpose for this is the binary graph Cl vs Na_2O (Figure 7), in which we have inserted both geological and archaeological samples.

The obsidians of Lipari, both geological and archaeological, stand at the centre of Figure 7, being characterised by intermediate values of both Cl (~0.30 wt %) and Na_2O (~4 wt %). Although the 152 archaeological samples belonging to this group were exposed for millennia to surface weathering processes, they appear compositionally quite compact, with only a few samples shifted toward the lower values of Na and Cl. Anyway, even the samples that deviate from the average values remain far from the other groups, without overlaps. The sub-sources of Gabellotto and Canneto Dentro cannot be differentiated in this graph.

Monte Arci group, represented only by geological samples, has Na_2O values of ~3–4 wt %, which partially superimpose to the Lipari values, but is clearly differentiated because of its lower Cl concentration (~0.10 wt %) (Figure 7). Within this group there is a tendency towards differentiation between the four sub-sources SA, SB1, SB2, and SC.

The Palmarola group appears to be well separated from both Lipari and Monte Arci, being characterised by higher Na values (~5 wt %) and intermediate Cl (~0.20 wt %).

Finally, the Pantelleria group plots in the upper right of Figure 7, characterised by high values of both Na_2O and Cl. This group shows a wide Cl dispersion; most samples belong to the southern obsidian sub-sources of Balata dei Turchi and Salto La Vecchia, characterised by average values of Na_2O between 6.50–7.50 wt % and Cl between 0.45−0.55 wt %. At lower values of Cl, there are the obsidians of the northern sub-source of Fossa della Pernice and the archaeological outlier UST-10 which, despite having a Cl (0.26 wt %) comparable with that of the Lipari obsidians, is clearly separated from them thanks to its high Na_2O content (7.42 wt %).

To sum up, the Cl vs. Na_2O plot sharply separates the four considered Central Mediterranean obsidian sources and resolves ambiguities and overlaps that may arise when relying only on major elements analyses. Equally effective for the provenance studies can be the binary graph Cl vs peralkalinity index (PI), while the others represented in Figure 6 do not guarantee the same spacing between the sources and exhibit a greater data dispersion.
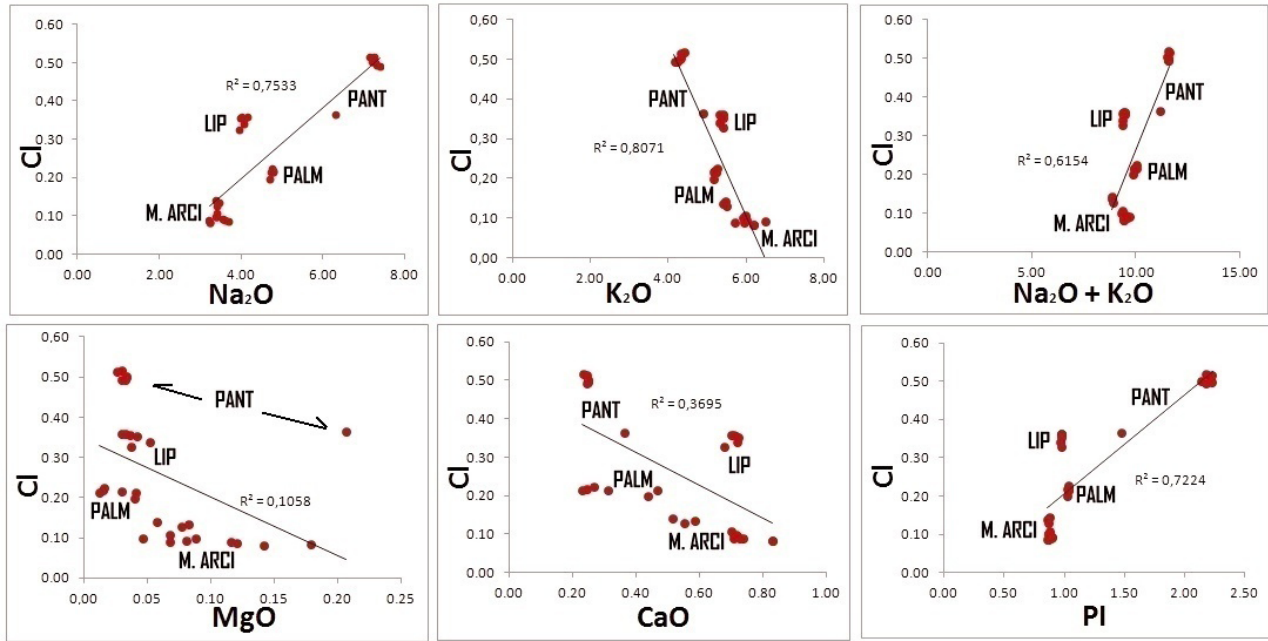
Figure 6: Correlations between chlorine and the main network modifying cations (Na, K, Mg, Ca), total alkali (Na_2O+K_2O) and peralkalinity index (PI), in the geological obsidian data set of this study.
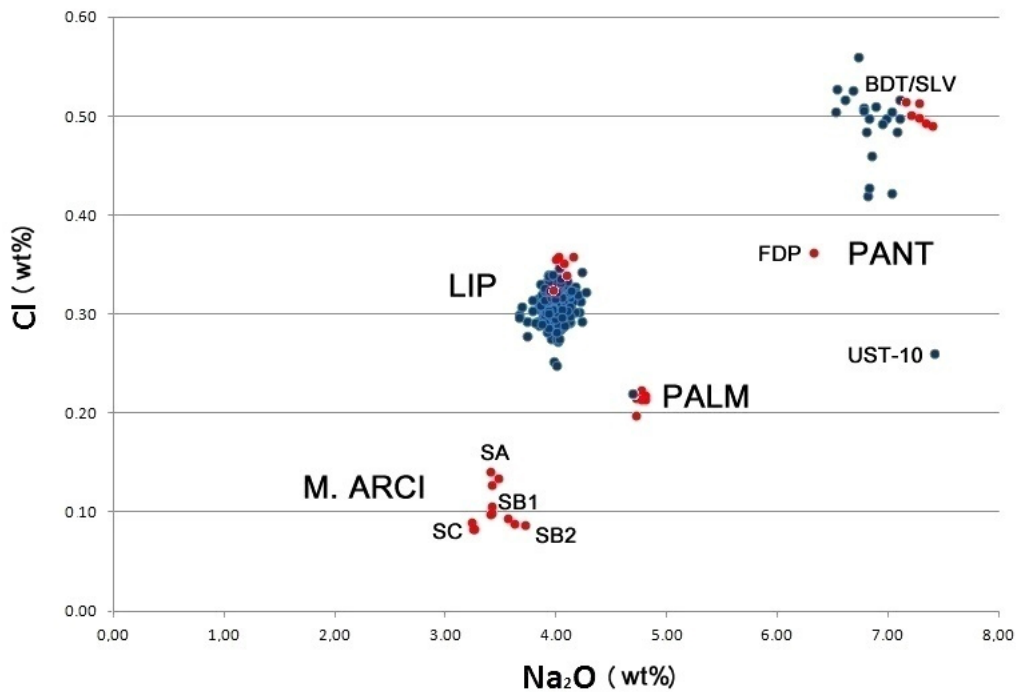

Figure 7: The binary Na_2O vs Cl graph selects unambiguously the four sources of obsidian from the Central Mediterranean. In the plot are inserted 31 geological samples (red dots) representative of the four obsidian sources: Monte Arci, Palmarola, Lipari, and Pantelleria; and 174 archaeological samples (blue dots) attributed to Lipari (152), Pantelleria (21) and Palmarola (1) (Foresta Martin et al., 2017). Abbreviations as in Figure 3. SA, SB1, SB2, SC are M. Arci sub-sources.

6 Conclusions

The geochemical characterisation of obsidian sources through rapid and low-cost analyses of a few major and minor elements is one of the primary objectives of archaeometric studies. Until now, chlorine has not been taken into consideration to characterise the four obsidian sources of the Central Mediterranean and it does not even appear in the chemical analyses that accompany most of the works on obsidians provenance.

In this paper, we demonstrate that Cl, although being a minor element present in volcanic glass in quantities < 1 wt %, has well-differentiated contents in the four obsidian sources exploited in the Central Mediterranean during prehistoric times, enough to be used as a reliable indicator of obsidian provenance. The efficacy of Cl for this purpose is enhanced when combined with Na, a chemical element that also discriminates obsidians of different origins and to which Cl is positively correlated.

This study is based on the analysis of a moderate number (31 samples) representative of the four Mediterranean obsidian sources, and of a considerable number (175) of archaeological samples of known provenance. Since obsidian analytical data with Cl content of the four Central Mediterranean obsidian outcrops are not available in the literature, we have not been able to extend our study to other groups of obsidian artifacts samples already chemically characterised, in order to validate and strengthen the effectiveness of our analytical elaborations. We suggest to authors who have analysed significant obsidian archeological assemblages, to reanalyse them including Cl, which is an element easily detectable with different analytical methods (SEM, EPMA, XRF), in order to further test its sources discriminating power.

References

Acquafredda, P., Andriani, T., Lorenzoni, S., & Zanettin, E. (1999). Chemical characterization of obsidians from different Mediterranean sources by non-destructive SEM-EDS analytical method. *Journal of Archaeological Science, 26*(3), 315–325. https://doi.org/10.1006/jasc.1998.0372

Acquafredda, P., & Paglionico, A. (2004). SEM-EDS microanalysis of microphenocrysts of Mediterranean obsidians: a preliminary approach to source discrimination. *European Journal of Mineralogy, 16*(3), 419–429. https://doi.org/10.1127/0935-1221/2004/0016-0419

Acquafredda, P., & Muntoni, I. M. (2008). Obsidian from Pulo di Molfetta (Bari, Southern Italy): provenance from Lipari and first recognition of a Neolithic sample from Monte Arci (Sardinia). *Journal of Archaeological Science, 35*(4), 947–955. https://doi.org/10.1016/j.jas.2007.06.017

Arias, C., Bigazzi, G., & Bonadonna, F. P. (1980). Studio cronologico e paleomagnetico di alcune serie sedimentarie dell'Italia apenninica. *Contributi preliminari alla realizzazione della Carta Neotettonica d'Italia*. Pub. no. 356 of the Geodynamic Finalized Program-Neotectonic Sub-Project, 1441–1448.

Barberi, F., Borsi, S., Ferrara, G., & Innocenti, F. (1967). Contributo alla conoscenza vulcanologica e magmatologica delle isole dell'Arcipelago Pontino. *Memorie della Societa Geologica Italiana, 6*, 581–606.

Barca, D., De Francesco, A. M., & Crisci, G. M. (2007). Application of Laser Ablation ICP-MS for characterization of obsidian fragments from peri-Tyrrhenian area. *Journal of Cultural Heritage, 8*(2), 141–150. https://doi.org/10.1016/j.culher.2006.12.001

Bellot-Gurlet, L., Bigazzi, G., Dorighel, O., Oddone, M., Poupeau, G., & Yegingil, Z. (1999). The fission-track analysis: An alternative technique for provenance studies of prehistoric obsidian artefacts. *Radiation Measurements, 31*(1-6), 639–644. https://doi.org/10.1016/S1350-4487(99)00157-2

Bigazzi, G., Bonadonna, F. P., Belluomini, G., & Malpieri, L. (1971). Studi sulle ossidiane italiane. IV. Datazione con il metodo delle tracce di fissione. *Bollettino della Società Geologica Italiana, 6*, 581–606.

Bigazzi, G., & Bonadonna, F. (1973). Fission track dating of the obsidian of Lipari Island (Italy). *Nature, 242*(5396), 322–323. https://doi.org/10.1038/242322a0

Bonifacie, M., Jendrzejewski, N., Agrinier, P., Humler, E., Coleman, M., & Javoy, M. (2008). The chlorine isotope composition of Earth's mantle. *Science, 319*(5869), 1518–1520. https://doi.org/10.1126/science.1150988 PMID:18339936

Bowen, N. L. (1937). Recent high-temperature research on silicates and its significance in igneous geology. *American Journal of Science, s5-33*(193), 1–21. https://doi.org/10.2475/ajs.s5-33.193.1

Burbidge, E. M., Burbidge, G. R., Fowler, W. A., & Hoyle, F. (1957). Synthesis of the Elements in Stars. *Reviews of Modern Physics, 29*(4), 547–650. https://doi.org/10.1103/RevModPhys.29.547

Cadoux, A., Pinti, D. L., Aznar, C., Chiesa, S., & Gillot, P. Y. (2005). New chronological and geochemical constraints on the genesis and geological evolution of Ponza and Palmarola volcanic islands (Tyrrhenian Sea, Italy). *Lithos, 81*(1-4), 121–151. https://doi.org/10.1016/j.lithos.2004.09.020

Cameron, A. G. (1973). Abundances of the elements in the solar system. *Space Science Reviews, 15*(1), 121–146. https://doi.org/10.1007/BF00172440

Cann, J. R., & Renfrew, C. (1964). The characterization of obsidian and its application to the Mediterranean region. *Proceedings of the Prehistoric Society, 30*, 111–133. https://doi.org/10.1017/S0079497X00015097

Carroll, M. R. (2005). Chlorine solubility in evolved alkaline magmas. *Annals of Geophysics, 48*(4-5), 619–630.

Carroll, M. R., & Webster, J. D. (1994). Solubilities of sulfur, noble gases, nitrogen, chlorine, and fluorine in magmas. In M. R. Carroll & J. R. Holloway (Eds.), *Volatiles in Magmas* (Reviews in Mineralogy & Geochemistry, Vol. 30, pp. 231–279). https://doi.org/10.1515/9781501509674-013

Clark, F. W., & Washington, H. S. (1924). *The composition of the earth's crust.* (Professional paper (Geological Survey (U.S.)), no. 127, pp. 8–16). Washington: Department of the Interior, United States Geological Survey.

Cornaggia Castiglioni, O., Fussi, F., & D'Agnolo, M. (1963). Indagini sulla provenienza dell'ossidiana utilizzata nelle industrie preistoriche del Mediterraneo occidentale. *Atti della Societa Italiana di Scienze Naturali e del Museo Civico di Storia Naturale in Milano, 102*, 310–322.

De Francesco, A. M., Crisci, G. M., & Bocci, M. (2008). Non-destructive analytic method using XRF for determination of provenance of archaeological obsidians from the Mediterranean area: A comparison with traditional XRF methods. *Archaeometry, 50*(2), 337–350. https://doi.org/10.1111/j.1475-4754.2007.00355.x

Donato, P., Barba, L., De Rosa, R., Niceforo, G., Pastrana, A., Donato, S., . . . Crisci, G. M. (2018). Green, grey and black: A comparative study of Sierra de las Navajas (Mexico) and Lipari (Italy) obsidians. *Quaternary International, 467*, 369–390. https://doi.org/10.1016/j.quaint.2017.11.021

Eggenkamp, H. (2014). *The geochemistry of stable chlorine and bromine isotopes.* Berlin: Springer. https://doi.org/10.1007/978-3-642-28506-6

Ewart, A. (1971). Chemical changes accompanying spherulitic crystallization in rhyolitic lavas, Central Volcanic Region, New Zealand. *Mineralogical Magazine, 38*(296), 424–434. https://doi.org/10.1180/minmag.1971.038.296.04

Foresta Martin, F., Di Piazza, A., D'Oriano, C., Carapezza, M. L., Paonita, A., Rotolo, S. G., & Sagnotti, L. (2017). New insights into the provenance of the obsidian fragments of the island of Ustica (Palermo, Sicily). *Archaeometry, 59*(3), 435–454. https://doi.org/10.1111/arcm.12270

Forni, F., Lucchi, F., Peccerillo, A., Tranne, C.A., Rossi, P. L., & Frezzotti, M. L. (2013). Stratigraphy and geological evolution of the Lipari volcanic complex (central Aeolian archipelago). In Lucchi, F. Peccerillo, A, Keller, J., Tranne, C. A., & Rossi, P. L. *The Aeolian Islands Volcanoes* (Memoirs Vol. 37, pp. 213–279). London: Geological Society. https://doi.org/10.1144/M37.10

Francaviglia, V. (1988). Ancient obsidian sources on Pantelleria (Italy). *Journal of Archaeological Science, 15*(2), 109–122. https://doi.org/10.1016/0305-4403(88)90001-5

Francaviglia, V. M. (2001). The search for a reliable discrimination between Mediterranean obsidians. *Proceedings of "Il vetro in Italia meridionale e insulare"* (pp. 5–7).

Gratuze, B. (1999). Obsidian characterization by laser ablation ICP-MS and its application to prehistoric trade in the Mediterranean and the Near East: Sources and distribution of obsidian within the Aegean and Anatolia. *Journal of Archaeological Science, 26*(8), 869–881. https://doi.org/10.1006/jasc.1999.0459

Glascock, M. D., Braswell, G. E., & Cobean, R. H. (1998). A systematic approach to obsidian source characterization. In Shackley M.S. (Eds.), *Archaeological Obsidian Studies* (Advances in Archaeological and Museum Science, Vol 3, pp. 15–65). Boston, MA: Springer. https://doi.org/10.1007/978-1-4757-9276-8_2

Hallam, B. R., Warren, S. E., & Renfrew, C. (1976). Obsidian in the western Mediterranean: Characterization by neutron activation analysis and optical emission spectroscopy. *Proceedings of the Prehistoric Society, 42*, 85–110. https://doi.org/10.1017/S0079497X00010719

Hanyu, T., Shimizu, K., Ushikubo, T., Kimura, J. I., Chang, Q., Hamada, M., . . . Ishikawa, T. (2019). Tiny droplets of ocean island basalts unveil Earth's deep chlorine cycle. *Nature Communications, 10*(1), 60. https://doi.org/10.1038/s41467-018-07955-8 PMID:30610195

Italiano, F., Correale, A., Di Bella, M., Foresta Martin, F., Martinelli, M. C., Sabatino, G., & Spatafora, F. (2018). The neolithic obsidian artifacts from Roccapalumba (Palermo, Italy): First characterization and provenance determination. *Mediterranean Archaeology & Archaeometry, 18*(3), 151–167. http://doi.org/10.5281/zenodo.1476967

Jarrad, R. D. (2003). Subduction fluxes of water, carbon dioxid, chlorine, and potassium. *Geochemistry, Geophysics, Geosystems, 4*, 8905. https://doi.org/10.1029/2002GC000392

Jordan, N. J., Rotolo, S. G., Williams, R., Speranza, F., McIntosh, W. C., Branney, M. J., & Scaillet, S. (2018). Explosive eruptive history of Pantelleria, Italy: Repeated caldera collapse and ignimbrite emplacement at a peralkaline volcano. *Journal of Volcanology and Geothermal Research, 349*, 47–73. https://doi.org/10.1016/j.jvolgeores.2017.09.013

Jwa, Y. J., Yi, S., Jin, M. E., Kasztovszky, Z., Harsányi, I., & Sun, G. M. (2018). Application of prompt gamma activation analysis to provenance study of the Korean obsidian artefacts. *Journal of Archaeological Science, Reports, 20*, 374–381. https://doi.org/10.1016/j.jasrep.2018.05.016

Kasztovszky, Z., & Biró, K. (2006). Fingerprinting Carpathian obsidians by PGAA: first results on geological and archaeological specimens. In *34th International Symposium on Archaeometry* (pp. 301–308). Centro de Estudios Borjanos.

Kasztovszky, Z., Biró, K. T., & Kis, Z. (2014). Prompt Gamma Activation Analysis of the Nyírlugos obsidian core depot find. *Journal of Lithic Studies, 1*(1), 151–163. https://doi.org/10.2218/jls.v1i1.784

Kasztovszky, Z., Biró, K. T., Nagy-Korodi, I., Sztáncsuj, S. J., Hágó, A., Szilágyi, V., . . . Mirea, P. (2019). Provenance study on prehistoric obsidian objects found in Romania (Eastern Carpathian Basin and its neighbouring regions) using Prompt Gamma Activation Analysis. *Quaternary International, 510*, 76–87. https://doi.org/10.1016/j.quaint.2018.12.020

Kuroda, P. K., & Sandell, E. B. (1953). Chlorine in igneous rocks: Some aspects of the geochemistry of chlorine. *Geological Society of America Bulletin, 64*(8), 879–896. https://doi.org/10.1130/0016-7606(1953)64[879:CIIR]2.0.CO;2

Lanzo, G., Landi, P., & Rotolo, S. G. (2013). Volatiles in pantellerite magmas: A case study of the Green Tuff Plinian eruption (Island of Pantelleria, Italy). *Journal of Volcanology and Geothermal Research, 262*, 153–163. https://doi.org/10.1016/j.jvolgeores.2013.06.011

Le Bourdonnec, F. X., Poupeau, G., & Lugliè, C. (2006). SEM–EDS analysis of western Mediterranean obsidians: A new tool for Neolithic provenance studies. *Comptes Rendus Geoscience, 338*(16), 1150–1157. https://doi.org/10.1016/j.crte.2006.09.018

Le Bourdonnec, F. X., Bontempi, J. M., Marini, N., Mazet, S., Neuville, P. F., Poupeau, G., & Sicurani, J. (2010). SEM-EDS characterization of western Mediterranean obsidians and the Neolithic site of A Fuata (Corsica). *Journal of Archaeological Science, 37*(1), 92–106. https://doi.org/10.1016/j.jas.2009.09.016

Le Maitre, R. W., Streckeisen, A., Zanettin, B., Le Bas, M. J., Bonin, B., Bateman, P., . . . Lameyre, J. (2002). Igneous Rocks: A Classification and Glossary of Terms. Recommendations of the International Union of Geological Sciences, Subcommission on the Systematics of Igneous Rocks. Cambridge University Press: Cambridge.

Lipman, P. W., Christiansen, R. L., & Alstine, R. E. V. (1969). Retention of alkalis by calc-alkalic rhyolites during crystallization and hydration. *American Mineralogist: Journal of Earth and Planetary Materials, 54*(1-2), 286–291.

Lowenstern, J. B. (1994). Chlorine, fluid immiscibility, and degassing in peralkaline magmas from Pantelleria, Italy. *The American Mineralogist, 79*, 353–369.

Macdonald, R., & Bailey, D. K. (1973). *The chemistry of the peralkaline oversaturated obsidians*. Washington, DC: US Gov.

Macdonald, R., Smith, R. L., & Thomas, J. E. (1992). *Chemistry of the subalkalic silicic obsidians*. Washington: U.S. G.P.O.

Maniar, P. D., & Piccoli, P. M. (1989). Tectonic discrimination of granitoids. *Geological Society of America Bulletin, 101*(5), 635–643. https://doi.org/10.1130/0016-7606(1989)1012.3.CO;2

Metrich, N., & Rutherford, M. J. (1992). Experimental study of chlorine in hydrous silicicmelts. *Geochimica et Cosmochimica Acta, 56*(2), 607–616. https://doi.org/10.1016/0016-7037(92)90085-W

Miyashiro, A. (1978). Nature of alkalic volcanic rock series. *Contributions to Mineralogy and Petrology, 66*(1), 91–104. https://doi.org/10.1007/BF00376089

Montanini, A., & Villa, I. M. (1993). 40Ar/39Ar chronostratigraphy of Monte Arci volcanic complex (western Sardinia, Italy). *Acta Vulcanologica, 3*, 229–233.

Palme, H., Lodders, K., & Jones, A. (2014). In M. Andrew (Ed.), *Solar system abundances of the elements. Planets, Asteriods, Comets and The Solar System, Treatise on Geochemistry* (2nd ed., Vol. 2, pp. 15–36). Davis: Elsevier.

Press, F., & Siever, R. (1978). *Earth*. San Francisco, California: WH Freeman & Company.

Radi, G., Bigazzi, G., & Bonadonna, F. (1972). Le tracce di fissione. Un metodo per lo studio delle vie di commercio dell'ossidiana. *Origini, 6*, 155–169.

Rotolo, S. G., Carapezza, M. L., Correale, A., Foresta Martin, F., Hahn, G., Hodgetts, A. G. E., . . . Speranza, F. (2020). Obsidians of Pantelleria (Strait of Sicily): A Petrographic, Geochemical and Magnetic Study of Known and New Geological Sources. *Open Archaeology, 6*(1), 434–453. https://doi.org/10.1515/opar-2020-0120

Rubey, W. W. (1951). Geologic history of sea water: An attempt to state the problem. *Geological Society of America Bulletin, 62*(9), 1111–1148. https://doi.org/10.1130/0016-7606(1951)62[1111:GHOSW]2.0.CO;2

Schilling, J. G., Unni, C. K., & Bender, M. L. (1978). Origin of chlorine and bromine in the oceans. *Nature, 273*(5664), 631–636. https://doi.org/10.1038/273631a0

Shand, S. J. (1927). *Eruptive Rocks*. New York: D. Van Nostrand Company.

Sharp, Z. D., & Draper, D. S. (2013). The chlorine abundance of Earth: Implications for a habitable planet. *Earth and Planetary Science Letters, 369*, 71–77. https://doi.org/10.1016/j.epsl.2013.03.005

Signorelli, S., & Carroll, M. (2002). Experimental study of Cl solubility in hydrous alkaline melts: constraints on the theoretical maximum amount of Cl in trachytic and phonolitic melts. *Contributions to Mineralogy and Petrology*, *143*(2), 209-218. https://doi.org/10.1007/s00410-001-0320-y

Tykot, R. H. (1992). The sources and distribution of Sardinian obsidian. In Tykot, R. H. & Andrews, T. K. (Eds.), *Sardinia in the Mediterranean: a footprint in the sea* (pp. 57–70). *Sheffield: Sheffield Academic Press.*

Tykot, R. H. (1995). Appendix I: obsidian provenance. In R.R. Holloway & S.S. Lukesh (Eds.), *Ustica I. The Results of the Excavations of the Regione Siciliana Soprintendenza ai Beni Culturali ed Ambientali Provincia di Palermo in Collaboration with Brown University in 1990 and 1991* (Archaeologia Transatlantica XIV, pp. 87–90). Providence, R.I.: Center for Old World Archaeology and Art, Brown University.

Tykot, R. H. (2002). Chemical fingerprinting and source tracing of obsidian: The central Mediterranean trade in black gold. *Accounts of Chemical Research, 35*(8), 618–627. https://doi.org/10.1021/ar000208p PMID:12186566

Tykot, R. H., & Young, S. M. M. (1996). Archaeological Applications of Inductively Coupled Plasma- Mass Spectrometry. In M. V. Orna (Ed.), *Archaeological Chemistry V* (pp. 116–130). Washington, DC: American Chemical Society. https://doi.org/10.1021/bk-1996-0625.ch010

Tykot, R. H., Setzer, T., Glascock, M. D., & Speakman, R. J. (2005). Identification and characterization of the obsidian sources on the island of Palmarola, Italy. *Geoarchaeological and Bioarchaeological Studies, 3*, 107–111.

Urey, H. C. (1951). The origin and development of the earth and other terrestrial planets. *Geochimica et Cosmochimica Acta, 1*(4-6), 209–277. https://doi.org/10.1016/0016-7037(51)90001-4

Williams-Thorpe, O. (1995). Obsidian in the Mediterranean and the Near East: A provenancing success story. *Archaeometry, 37*(2), 217–248. https://doi.org/10.1111/j.1475-4754.1995.tb00740.x

Webster, J. (1997). Chloride solubility in felsic melts and the role of chloride in magmatic degassing. *Journal of Petrology, 38*(12), 1793–1807. https://doi.org/10.1093/petroj/38.12.1793

Winterton, N. (2000). Chlorine: The only green element–towards a wider acceptance of its role in natural cycles. *Green Chemistry, 2*(5), 173–225. https://doi.org/10.1039/b003394o

Zanchetta, G., Sulpizio, R., Roberts, N., Cioni, R., Eastwood, W. J., Siani, G., . . . Santacroce, R. (2011). Tephrostratigraphy, chronology and climatic events of the Mediterranean basin during the Holocene: An overview. *The Holocene, 21*(1), 33–52. https://doi.org/10.1177/0959683610377531